

Dynamic compressive behaviour of recycled tyre steel fibre reinforced concrete

Meng Chen^a, Hanqing Si^a, Xiaochun Fan^b, Yiwei Xuan^c, Mingzhong Zhang^{c,*}

^a *School of Resources and Civil Engineering, Northeastern University, Shenyang 110819, China*

^b *School of Civil Engineering and Architecture, Wuhan University of Technology, Wuhan 430070, China*

^c *Department of Civil, Environmental and Geomatic Engineering, University College London, London WC1E 6BT, UK*

Abstract: This paper presents a systematic experimental study on dynamic compressive behaviour of recycled tyre steel fibre (RTSF) reinforced concrete. The use of RTSF can not only enhance the mechanical properties and sustainability of cementitious materials but also reduce the environmental impact of waste tyres. A series of tests were conducted to investigate the effect of RTSF content (0.5%, 0.75%, 1.0% and 1.25%) on workability, air content and compressive strength of concrete as well as the dynamic compressive behaviour under various impact velocities (35, 55, 75, 95, 110 and 125 s⁻¹). For comparisons, plain concrete without fibre and concrete reinforced with 1.0% industrial steel fibre (ISF) were regarded as the reference mixtures. The split Hopkinson pressure bar (SHPB) was adopted to study the dynamic failure pattern, dynamic compressive strength, dynamic increase factor (DIF), energy dissipation and toughening mechanism. Results indicate that with increasing RTSF content, the slump of concrete was reduced while its air content was increased. At the same fibre content (1.0%), RTSF reinforced concrete exhibited a higher workability and air content than ISF reinforced concrete due to the different fibre shape and aspect ratio. The compressive strength of concrete at various strain rates went up with the increase of RTSF content from 0 to 0.75% but reduced with the further increase of RTSF content from 0.75% to 1.25%. DIFs of all mixtures were closely related to strain rate. The optimal dosage of RTSF for concrete was found to be 0.75%, considering workability, compressive strength, and dynamic compressive performance.

Keywords: Fibre reinforced concrete; Recycled fibre; Split Hopkinson pressure bar; Dynamic properties; Impact behaviour; Toughening mechanism

* Corresponding author. E-mail address: mingzhong.zhang@ucl.ac.uk (M. Zhang)

1. Introduction

Concrete is the most widely used man-made material in the world, but it is brittle and prone to cracking when subjected to tensile and shrinkage forces. To tackle this issue, discrete fibres such as steel, glass, synthetic and natural fibres are usually incorporated into concrete to form fibre reinforced concrete (FRC) and enhance the strengths and toughness of concrete [1, 2]. For instance, concrete containing randomly dispersed steel fibres with different geometries and shapes exhibits superior compressive, flexural and splitting tensile strengths, crack resistance and durability [3-6]. However, in the context of a growing demand for sustainable and innovative development of building materials, an increasing number of studies have attempted to replace the steel fibres in concrete with recycled materials, e.g., end-of-life tyres [7-9].

It was reported that about 1.5 billion waste tyres are produced every year [10], many of which need to be buried, landfilled, and stockpiled and thus could threaten the environment [9]. The addition of recycled waste tyre components into concrete can help reduce such environmental impact and enhance sustainability and properties of concrete [11-13]. For instance, waste tyre rubber particles can be used as alternative aggregates for cementitious composites [8, 14-16], while steel wires derived from waste tyres which are usually referred to as ‘recycled tyre steel fibre (RTSF)’ can be used to partially or fully replace the commonly used industrial steel fibres in FRC [2, 17-19].

In recent years, several studies have been carried out to investigate the engineering properties of RTSF reinforced concrete. The emphasis is placed on the mechanical properties of concrete reinforced with hybrid RTSF and industrial steel fibre (ISF) to examine the feasibility of replacing ISF with RTSF [2, 17, 20-26]. It was reported that RTSF had similar effects as ISF on the compressive strength of concrete with a certain fibre dosage, and the tensile strength and ductility of RTSF reinforced concrete can be even higher as compared with ISF reinforced concrete with acceptable shear performance [24]. The tensile strength of 1% RTSF reinforced concrete can be enhanced by 49-68% in comparison with plain concrete [19]. In terms of durability, concrete reinforced with RTSF exhibits a slight corrosion susceptibility compared to ISF reinforced concrete while it does not obviously decrease the post-cracking resistance [27], which is consistent with the findings by Centonze et al. [28] and Caggiano et al. [2] that the addition of RTSF can significantly reduce the brittle characteristics of concrete and bring comparable post-cracking behaviour compared to ISF reinforced concrete. Besides, the effects of RTSF features including geometrical dimensions and pull-

out behaviour were also investigated. It was found that RTSF could provide a stronger adhesive force between matrix and fibre [18]. Regarding the pull-out behaviour of fibres, although a considerable improvement in flexural behaviour can be found in RTSF reinforced concrete compared to plain concrete, the post-cracking behaviour of FRC could be poorer by replacing ISF with RTSF due to lower efficiency and higher aspect ratio, suggesting that it is crucial to use an appropriate amount and aspect ratio of RTSF [2, 17, 18, 28]. The fibre length and impurities would also affect the mechanical performance of RTSF reinforced concrete. Very short RTSF cannot provide sufficient anchorage length to develop strength, while the workability of FRC can be decreased with the addition of longer RTSF [29]. On the other hand, the effect of RTSF content on engineering properties of FRC has been gradually studied [18, 22, 27, 30-32]. The flexural stiffness, toughness, and structural behaviour of FRC were enhanced with the increase of RTSF content within a certain range. However, a larger amount of RTSF may have a negative effect on workability and static compressive strength. Hu et al. [22] presented a systematic experimental study on the mechanical properties of FRC containing various contents of hybrid ISF and RTSF and found that the critical RTSF dosage was within 30 kg/m^3 , while RTSF with 10 kg/m^3 dosage resulted in the best synergetic effect. Micro-cracks can also be controlled more effectively after adding RTSF. Compared to other common fibres, previous studies illustrated that the incorporation of RTSF can lead to better mechanical performance. For instance, concrete reinforced with hybrid RTSF and polypropylene (PP) fibres, the further incorporation of RTSF resulted in higher compressive strength and flexural strength in comparison with PP fibre [33]. Besides, compared with the effect of recycled tyre steel cord (RTSC) that is also recycled from waste tyres, although RTSF reinforced ultra-high performance concrete had slightly lower workability, compressive strength and elastic modulus, its cost and environmental efficiency were 48%-80% and 69%-135% beyond RTSC reinforced concrete [29].

Recently, the static mechanical properties, durability, and sustainability of RTSF reinforced concrete have been extensively studied, while the dynamic behaviour of concrete reinforced with RTSF has been rarely explored. It is worth noting that the concrete structures in service would be subjected to not only static loading, but also dynamic loads such as earthquakes, blasts, explosions, and projectile impact [34]. The dynamic compressive behaviour of RTSF reinforced concrete is significant for their applications in earthquake, coastal, and critical infrastructure protection regions. Moreover, the strain rate has a significant effect on dynamic mechanical properties of concrete [35-

39]. Thus, it is vital to investigate the effects of strain rate and fibre dosage on dynamic compressive behaviour of RTSF reinforced concrete, and the feasibility of replacing ISF with RTSF to enhance dynamic compressive properties and sustainability of concrete, which have not been addressed elsewhere.

The main purpose of this study is to investigate the dynamic compressive behaviour of RTSF reinforced concrete considering various strain rates and fibre dosages (0.5%, 0.75%, 1.0% and 1.25% by volume). For comparisons, concrete reinforced with 1.0% ISF and plain concrete without fibre were regarded as the reference mixtures. A series of tests were conducted to estimate the effect of RTSF content on workability, air content and static compressive strength of concrete as well as the dynamic compressive behaviour under various impact velocities using split Hopkinson pressure bar (SHPB) in terms of dynamic failure pattern, dynamic compressive strength, dynamic increase factor (DIF) and energy dissipation. Afterwards, the toughening and failure mechanisms of RTSF reinforced concrete were explored with the assistance of a portable electron microscope. Finally, an optimal dosage of RTSF for concrete considering the static and dynamic mechanical properties was proposed.

2. Experimental program

2.1 Raw materials

P.O. 42.5 ordinary Portland cement with a specific gravity of 3.09 was used in this study, the chemical composition of which is shown in Table 1. Natural river sands with a specific gravity of 2.56, a nominal maximum size of 4.75 mm and fineness modulus of 2.89 were used as fine aggregates, the particle size distribution of which is presented in Table 2. Coarse aggregates were crushed granites with particle sizes in the range of 5-10 mm, the properties of which are given in Table 3. Polycarboxylate-based superplasticisers (SPs) with a density of 4 kg/m³ were added during mixing process to improve the workability of concrete specimens.

RTSF and ISF were adopted as reinforcement. RTSF was supplied by a Chinese tyre recycling company, Jinghan rubber and plastic products Co. Ltd in Shanghai. Given that these RTSF had irregular geometries and corrugated shapes, the distance between the outer ends of RTSF was defined as fibre length [24, 28]. Fig. 1 shows the length distribution of RTSF that was obtained based on 1000 RTSFs. The average length of RTSF was 7.3 mm, while the minimum and maximum lengths were 1.4 mm and 15.6 mm, respectively. The ratio between the average developed length and nominal length was 1.32. Dramix 3D 65/35BG hooked-end steel fibre was used as ISF, manufactured by

Chinese Bekaert Co. Ltd in Shanghai. The physical and mechanical properties of RTSF and ISF are illustrated in Table 4.

2.2 Mix proportions

To study the influence of fibre type (ISF and RTSF) and fibre content (0.5%-1.25%) on the dynamic compressive performance of concrete the mix proportions of concrete specimens were designed and presented in Table 5. The numbers '0.5', '0.75', '1.0', and '1.25' represent the corresponding fibre dosage of each specific fibre. For instance, '0.5' means the fibre volume fraction was 0.5%. RTSF0 refers to plain concrete without steel fibres. It was suggested that the volume fraction of ISF in ordinary concrete should be controlled within 0.5%-1.5% [40] and when the volume fraction of RTSF reached 1.25%, the workability of concrete became worse, and its compressive strength would be declined by 5% [2]. Thus, the upper limit of the incorporated RTSF dosage was determined as 1.25%. Previous studies [41, 42] demonstrated that the static compressive strength and splitting tensile strength of concrete could be effectively increased with the addition of 0.75% RTSF. Moreover, incorporating 0.75% RTSF can obviously improve the flexural strength and energy absorption capability of concrete, while for lightweight aggregate concrete, the impact resistance can be enhanced by 10-18 times [43]. In addition, when the volume fraction of ISF with length of 35 mm and aspect ratio of 65 reached 1.0%, the concrete exhibited better workability and mechanical properties [44]. However, the effect of the above-mentioned RTSF content (0.5%-1.25%) on dynamic compressive properties of concrete at high strain rates (around 100 s^{-1}) has not been investigated. Thus, in this study, concrete specimens with four RTSF dosages ranging from 0.5% (39 kg/m^3) to 1.25% (98 kg/m^3) were designed to explore the static and dynamic compressive performance, in comparison with plain concrete without steel fibre and concrete containing 1.0% ISF. The aim is to verify the feasibility of replacing ISF with RTSF and determine the optimal content of RTSF for concrete considering the static and dynamic mechanical properties. Also as shown in Table 5, the water-to-binder (w/b) ratio was kept as 0.42 and the design compressive strength of concrete was 40 MPa.

2.3 Sample preparation

Regarding the mixing process, dry materials including fine and coarse aggregates and cement were first dry mixed for about 2 min. Then SPs and water were added and mixed for no less than 2 min, followed by the gradual addition of fibres until a uniform fibre distribution. After the mixing process,

fresh concrete mixtures were casted into different moulds and vibrated on a vibration. Afterwards, the specimens were placed for 24 h before being de-moulded and then cured in a standard curing room (20 ± 2 °C and 95% RH) for 7 or 28 d. The end faces of the cylinder specimens used for dynamic test should be worn flat to ensure that the error of non-parallelism between the two end faces was no more than 0.1 mm, and the deviation between the end faces and the axis was no more than 0.25° . The test design and number of specimens are summarised in Table 6.

2.4 Test methods

2.4.1 Slump test

Slump test was conducted for all mixtures to study the effect of fibre on workability of concrete according to GB/T50080-2016 [45]. The concrete mixtures were evenly added into the specified slump cone with the size of $100 \times 200 \times 300$ mm in three layers. The height of the mixtures in each layer was about $1/3$ of the cylinder height. After each filling, the concrete mixture samples were evenly jolted from the edge to the centre with a tamping rod for 25 times in a spiral manner. Afterwards, the excess concrete mixture was scraped off and smoothed along the top of the cone, followed by pulling out the slump cone vertically from bottom to top. Finally, to determine the slump value of the specimens, the vertical displacement difference between the top surface of the cone and the highest point of the samples after the slump shall be measured after samples have been standing for 30 s.

2.4.2 Air content test

The air content of all fresh concrete mixtures was measured in accordance with GB/T50080-2016 [45] using the Type LC-615A air entrainment meter. Each fresh mixture was first added into the air entrainment meter and tested twice, and the air content of the mixture can be calculated according to the following equation.

$$A = A_0 - A_g \quad (1)$$

where A is the actual air content of concrete mixture (%), A_0 is the uncorrected air content of concrete mixture shown by the air entrainment meter, and A_g is the air content of aggregates (%).

If the difference between the two test results is no more than 2%, the final air content value of the mixture shall be the average of the two calculated results.

2.4.3 Static compressive strength test

Static compressive strength tests were conducted on three 150 mm concrete cubic specimens as per GB/T50081-2002 [46] at 7 and 28 d for each mixture using an electro-hydraulic servo pressure testing machine (1000 kN) with a constant loading rate at 10 MPa/s. During this process, the pressure surface of the specimens was placed vertically with the top surface when forming to ensure the centre of the specimen is aligned with the centre of the lower pressure plate of the testing machine.

2.4.4 Dynamic compressive strength test

As illustrated in Fig. 2, dynamic compressive strength test was conducted on concrete cylinder specimens with size of 100 × 50 mm using a 100 mm split Hopkinson pressure bar (SHPB), the main components of which include a 600 mm length striker bar, a 5000 mm length incident bar, a 3500 mm length transmitted bar and a 1200 mm length absorbing bar. All these bars are made of high-strength alloy steel. The auxiliary components contain launching devices, speed detection devices, strain collecting devices and an absorber. The impact velocities of the striker bar were set as about 5.2, 7.4, 8.5, 9.4, 10.6 and 11.6 m/s respectively by adjusting the nitrogen pressure and the striker bar depth. It is worth mentioning that the strain rate of the specimens increased with the increase of striker bar velocity. Taking RTSF0 as an example, the relationship between the average strain rate (35.0-125.5 s⁻¹) and the striker bar speed (5.2-11.6 m/s) is shown in Fig. 3.

Before the test, the two contact surfaces between the specimen and the bars should be smeared with Vaseline to avoid the end friction effects. When the test began, the pressure of the inflator reached a set value, and then the valve was activated, allowing the compressed nitrogen to drive the striker bar into the incident bar. The incident wave ($\varepsilon_i(t)$) was first generated in the incident bar due to the high impact. Then, a reflected pulse known as reflected wave ($\varepsilon_r(t)$) was subsequently transformed from part of the incident wave at the contact surface between the incident bar and the tested specimen, while the remaining incident wave continued to propagate forward through the specimen into the transmitted bar to form the transmitted wave ($\varepsilon_t(t)$). During the impact process, two strain gauges were attached on incident and transmitted bars, which were placed 2500 mm respectively from the end of the specimen for real-time strain pulse recording.

The principle of SHPB test is based on the propagation theory and stress uniformity assumption of one-dimensional waves in the elastic bars [47]. In order to prove stress uniformity of the specimens during the test, a pulse shaper with a diameter of 50 mm and a thickness of 2 mm was attached on the

incident bar to transform the waveform. The pulse shaper can not only weaken the shock of the wave through the plastic deformation after the impact to minimise the dispersion effect in the test [48], but also prolong the rising time of the incident pulse to ensure the stress equilibrium inside the tested specimens [49]. As shown in Fig. 4, the incident wave combined with the reflected wave approximately equals the transmitted wave, indicating that the stress equilibrium was achieved, which follows:

$$\sigma_t = \sigma_i + \sigma_r \quad (2)$$

where σ_t is the incident stress (MPa), σ_i represents the transmitted stress (MPa), and σ_r is the reflected stress (MPa).

With the assumption of one-dimensional propagation of stress wave and uniform stress of specimen, the three-wave method was adopted to process the test data. Stress $\sigma_s(t)$, strain $\varepsilon_s(t)$ and strain rate $\dot{\varepsilon}_s(t)$ can be calculated as follows:

$$\begin{cases} \sigma_s(t) = \frac{EA_0}{2A_s} [\varepsilon_i(t) + \varepsilon_r(t) + \varepsilon_t(t)] \\ \varepsilon_s(t) = \frac{C_0}{l_s} \int_0^t [\varepsilon_i(t) - \varepsilon_r(t) - \varepsilon_t(t)] dt \\ \dot{\varepsilon}_s(t) = \frac{C_0}{l_s} [\varepsilon_i(t) - \varepsilon_r(t) - \varepsilon_t(t)] \end{cases} \quad (3)$$

where E is the elastic modulus of the bars (MPa), A_0 and A_s represents the cross-sectional area of the bars (mm^2) and the tested specimen (mm^2), respectively, C_0 denotes the elastic wave velocity in the bars (m/s), and l_s is the thickness of the tested specimen (mm).

The cracks caused by impact and the distribution of steel fibres in concrete specimens can be observed and analysed using the portable digital electron microscope.

3. Results and discussion

3.1 Slump

Fig. 5 displays the slump values of all mixtures, indicating a reduction in slump of concrete with the increase of RTSF content. Compared to that of the reference mix RTSF0 (155 mm), the slump of RTSF0.5, RTSF0.75, RTSF1.0, RTSF1.25 was decreased by 14.8%, 21.9%, 25.8%, 32.9%, respectively. Hence, under the condition of constant w/b ratio and the SP dosage, the incorporation of RTSF reduced the workability of concrete [18, 50, 51], which is similar to the effect of industrial steel fibre on workability of concrete [52]. This can be attributed to higher surface area of elongated

steel fibre compared with aggregates at the same volume, resulting in increased cohesive forces between the fibre and matrix. Besides, the granular fabric structure could be altered by fibres, which also separated the particles apart [53]. Moreover, steel fibres could be disorderly distributed in the mixtures, thereby hindering the flow of concrete [51]. As seen in Fig. 5, previous studies demonstrated that when the RTSF content raised from 0 to 0.46%, the slump of RTSF reinforced concrete was reduced by 33.3% [51], and the slump of RTSF reinforced concrete with 1.0% RTSF was 58.2% lower than that of plain concrete [50]. Thus, the fibre morphology and length distribution of RTSF have a significant effect on workability of concrete.

It can be clearly observed that for the same fibre volume fraction (1.0%), the effect of ISF on concrete slump was more significant than that of RTSF. This can be explained as follows: (1) The length of RTSF was generally smaller than that of ISF, which reduced the resistant forces to flow for mixtures in comparison with ISF whilst mixing; (2) RTSFs with different lengths were mixed together, leading to more restriction on rotation to each other than ISF. Hence, RTSF could avoid being perpendicular to the flow direction throughout the mixing process, which reduced the resistance to flow [47, 53]; (3) As hooked-end fibre, ISF could improve the cohesive forces between steel fibre and concrete and inhibit the flow of concrete. Consequently, replacing ISF with RTSF could improve the slump of concrete and increase the compactness of concrete, thereby reducing the negative effect of steel fibres on mechanical properties of concrete. According to JGJT-2019 [54], when the pumping height reaches 30 m, the slump of the pumped concrete needs to be 100-140 mm. In this experiment, the slump of concrete containing 0.5%-1.0% RTSF exceeded 100 mm, suggesting that the workability met the pumping requirements.

3.2 Air content

Fig. 6 shows the air content of concrete with various volume fractions of RTSF and ISF. An obvious trend can be found that the air content of RTSF reinforced concrete was increased with increasing RTSF dosage, where the air content of RTSF0.5, RTSF0.75, RTSF1.0 and RTSF1.25 was raised by 12.5%, 38.8%, 54.2% and 71.5%, respectively compared to that of RTSF0. This can be ascribed to the weak interface between fibre and matrix induced by RTSF in the mixtures, leading to more access for entrapping air. During the mixing process, the addition of fibres could entrap more air and thus increase the air content of mixtures [55, 56]. Also, it is worth noting that the air content was reduced with the increase of slump of concrete. With the increase of workability of concrete mixtures, the air

in the mixtures was easier to seep outward and the air content decreased accordingly [57]. As seen in Fig. 6, the air content of ISF1.0 was increased by 15.3% as compared with RTSF1.0 under the same fibre content, which agrees well with previous studies [23, 58] that the air content of concrete with 0.3% ISF dosage was about 11.1% higher than that of concrete with the same RTSF dosage. Besides, the aspect ratio of ISF was 65, while the proportion of RTSF with aspect ratio of lower than 65 was 96.9%. This is consistent with previous studies [23, 58] that concrete containing hooked-end FRC (1.0%) with aspect ratio of 80 exhibited an approximately 66.7% higher air content than the same type concrete with aspect ratio of 60.

3.3 Static compressive strength

Fig. 7 illustrates static compressive strength of different concrete specimens at 7 d and 28 d. It can be observed that with the increase of RTSF content, the compressive strength of RTSF reinforced concrete showed a decreasing trend after the first increase. The static compressive strength of RTSF0.5, RTSF0.75, RTSF1.0 and RTSF1.25 at 7d was 3.8%, 15.9%, 13.0% and 7.5% respectively higher than that of RTSF0, which was 41.6 MPa. Similarly, when the curing age was 28 d, the static compressive strength of RTSF0.5, RTSF0.75, RTSF1.0 and RTSF1.25 was 3.2%, 15.0%, 12.6% and 5.4% higher respectively than that of RTSF0 (i.e., 50 MPa). It can be found that concrete reinforced with 0.75% RTSF had the highest static compressive strength. Fig. 8 shows the relative compressive strength that is defined as the ratio of compressive strength of RTSF concrete with different fibre dosages to that of plain concrete without fibre. It should be noted that the optimal fibre dosage appeared at 0.23% [18], 0.46% [51] and 0.75% [41], respectively, suggesting that the effect of fibre is dependent on the difference in fibre length distribution and strength of concrete matrix.

The bond between fibre and concrete matrix is mainly determined by the chemical bond, the mechanical anchoring force between both ends of the fibre and interface, and the friction between fibre and concrete matrix [59]. Hence, the effect of RTSF on static compressive strength of concrete can be associated with the bond produced by RTSF and concrete matrix. When the internal cracks of concrete began to propagate during the compression process, RTSF tightly bonded to concrete matrix and thus significantly delay the propagation of cracks [28]. However, when the RTSF dosage was high (1.0-1.25%), the compressive strength of RTSF reinforced concrete was decreased. This can be explained by the fact that: (1) Compared with RTSF0.75, the slump of RTSF1.0 and RTSF1.25 slump was decreased by 5.2% and 14.1%, and their air content was increased by 11.0% and 23.5%,

respectively. With the increase of RTSF content, more mortar in concrete was driven to wrap more fibres, leading to the decrease in the compactness and the bond between fibre and concrete matrix as well as the compressive strength of concrete [60, 61]; (2) The addition of RTSF weakened the interfacial zone and thus increased the defects in concrete mixtures.

3.4 Dynamic failure patterns

The failure patterns of all concrete mixtures under dynamic compression are illustrated in Table 7. Different from the failure of concrete under static compression, with the increase of strain rate from 35 s^{-1} to 125 s^{-1} under dynamic loading, the failure patterns of most mixtures (apart from RTSF0) exhibited similar characteristics, changing from almost no damage to core-integrity failure. For RTSF0, further pulverization failure could occur when the strain rate reached 125 s^{-1} , as seen in the failure patterns of RTSF0 at 125 s^{-1} in Table 7. In addition, the damage level of concrete increased with the increase of strain rate, which is consistent with the findings presented in [49, 62-64] that more complete and larger elements can be observed in the specimens at a low strain rate, whereas at a high strain rate the number of micro-cracks and macro-cracks increased and the specimen was broken into smaller fragments, which can be attributed to the short impact time. As a result, the internal micro-cracks in concrete did not have sufficient time to grow, nevertheless more cracks were generated. When the strain rate was around 35 s^{-1} , all specimens were basically not damaged, while the edges of various specimens appeared slight tensile failure when the strain rate was about 55 s^{-1} , and the cracks developed from the edge to the interior of the specimen as the strain rate was increased to near 75 s^{-1} . In comparison with edge cracking and spalling failure occurred in RTSF0 and RTSF0.5 specimens, only a few large fragments appeared on the outside of ISF1.0, RTSF1.0 and RTSF1.25 and only a slight tensile failure occurred in RTSF0.75. As the increase of strain rate to $95\text{-}110 \text{ s}^{-1}$, the outer area of the concrete specimen was broken, followed by the fibre debonding and fibre pull-out of the concrete matrix, but the core area kept complete. With the further increase of strain rate to around 125 s^{-1} , RTSF0 specimen was broken into loose particles and pulverization failure appeared, whilst the cracks in RTSF and ISF reinforced concrete developed towards the middle area. Afterwards, more fibres were pulled out, while some fragments were bridged by the fibres. Meanwhile, the size of the fragments decreased along with the increasing number of fragments, whereas RTSF and ISF reinforced concrete still preserved the integrity of core-area. In addition, the fibres at the cracks can be observed to pull out or bridge the fractured pieces, as seen in Fig. 9. The bond strength between

fibre and concrete was lower than tensile strength of fibre, making the fibres easier to pull out than to rupture, which agrees well with the findings presented in [65]. Besides, during the dynamic compression process, the damage of specimen extended from the outside to the inside as the internal concrete was constrained by the external concrete, and the cracks gradually propagated through the core concrete with the increase of strain rate.

As seen in Table 7, the fragments of RTSF0 were significantly more than that RTSF reinforced concrete at various strain rates, which suggests that under impact loading a certain amount of RTSF can effectively prevent the initiation and propagation of cracks and limit the transverse deformation, thereby enhancing the dynamic resistance of concrete. In addition, it can be observed that under the same strain rate, the concrete specimens containing 0.75% RTSF exhibited the best resistance to damage under dynamic compression.

3.5 Dynamic compressive strength

3.5.1 Effect of strain rate

Fig. 10 shows the effect of strain rate varying from around 34.9 s^{-1} to 127.2 s^{-1} on dynamic compressive stress-strain curve of all concrete mixtures at 28 d. The stress-strain curves of different mixtures indicated the same trend, consisting of a linear ascending region, a plastic region due to the initiation and propagation of micro-cracks in concrete from the outside to the inside, and a softening region after the peak stress was reached, where the cracks in concrete further propagated and finally the concrete was destroyed [65-67]. The failure patterns can be found in Table 7.

The effect of strain rate on dynamic compressive strength of RTSF and ISF reinforced concrete is demonstrated in Fig. 11, which indicates that the dynamic compressive strength was increased with the increase of strain rate. As the strain rate increased from 34.9 s^{-1} to 127.2 s^{-1} , the dynamic compressive strength of RTSF0, RTSF0.5, RTSF0.75, RTSF1.0 and RTSF1.25 was enhanced by 6.8-76.7%, 8.6-71.1%, 7.1-70.9%, 8.0-72.9%, 8.2-73.4% and 5.8-72.1%, respectively. This can be ascribed to the strain rate effect of FRC under dynamic loading, i.e., the lateral inertial effect of the specimen surface caused the increase of compressive strength in dynamic compression tests. Additionally, as per the system energy balance theory under high-speed impact, the energy required to generate cracks was far higher than that needed for cracks to propagate [68, 69], leading to the rapidly increasing number of micro-cracks under high strain rate. Meanwhile, the interior of concrete did not have enough time to accumulate energy and resist deformation. Instead, the internal stress

was increased and thus the energy absorption was enhanced against impact loadings [70]. The rapid propagation of cracks due to high-speed impact improved the bond between fibres and matrix, leading to better reinforcement performance of fibres in concrete. Also, free water flowed in the voids of concrete when concrete is subjected to dynamic loading, resulting in resistance to the growth of micro-cracks, which is known as the Stefan effect [71]. The growth rate of dynamic compressive strength of RTSF reinforced concrete was decreased with the increase of strain rate. The growth rate ranges of concrete containing various RTSF contents at two adjacent strain rates are 71.1-76.9% (35-55 s⁻¹), 24.3-30.7% (55-75 s⁻¹), 15.4-19.3% (75-95 s⁻¹), 13.2-14.9% (95-110 s⁻¹) and 6.2-10.4% (110-125 s⁻¹), respectively. The number of cracks in concrete under high-speed impact was increased, reducing the bond length of RTSF in concrete and thus further decreased the bridging action of RTSF in concrete matrix [64]. Moreover, the increasing strain rate enlarged the crack width of concrete, followed by decreasing bonding area between RTSF and concrete matrix. Hence, the effect of RTSF on the dynamic compressive strength of concrete was reduced.

Table 8 illustrates the strain at peak stress and ultimate strain, which can reflect the deformation capacity of concrete under dynamic loading. It can be found that the ability of concrete to resist deformation was improved with increasing strain rate. In this study, the ultimate strain of different concrete mixtures was about 1.5 times the strain at peak stress. Both the strain at peak stress and ultimate strain were increased with the increase of strain rate, which can be attributed to the inhomogeneity in the interior of concrete [72]. With the increase of strain rate from 35 s⁻¹ to 55 s⁻¹, the ultimate strain presented the largest growth range, where the ultimate strain of different concrete mixtures was increased, with a range from 40.3% to 70.1%, while it was decreased significantly with the further increase of strain rate. As the strain rate was raised from 110 s⁻¹ to 125 s⁻¹, the growth range of ultimate strain was only 6.8-16.3%. The bridging action of fibre at the cracks of concrete enlarged the strain-softening zone and thereby enhanced the toughness of concrete.

3.5.2 Effect of RTSF content

Fig. 12 shows the effect of RTSF content on dynamic compressive strength of concrete at different strain rates. The incorporation of RTSF (0.5-1.25%) could improve the dynamic compressive strength of concrete. The dynamic compressive strength of RTSF0.5, RTSF0.75, RTSF1.0 and RTSF1.25 under different strain rates (from 34.9 s⁻¹ to 127.2 s⁻¹) was increased by 5.5-9.7%, 17.6-25.1%, 13.5-20.8% and 7.2-15.3%, respectively. The dynamic compressive strength of concrete was increased

with the increase of RTSF content and reached the maximum when the RTSF dosage was 0.75%, and then decreased with the further addition of RTSF. As compared with RTSF0, the dynamic compressive strength of RTSF0.75 was increased by 21.5%, 17.6%, 19.8%, 24.8%, 25.1%, and 23.0%, respectively, at the average strain rates of 34.9 s^{-1} , 54.3 s^{-1} , 75.4 s^{-1} , 93.3 s^{-1} , 110.9 s^{-1} and 124.9 s^{-1} . The dynamic compressive strength of RTSF1.0 and RTSF1.25 at different strain rates was decreased by 3.5-5.4% and 6.0-9.9% in comparison with RTSF0.75, indicating a similar trend to static compressive strength. This reduction in efficiency with the addition of RTSF can be ascribed to the reduced workability, increased air content and decreased compactness of concrete. In addition, the uniformity of fibre distribution became worse, and the bridging action between fibre and concrete matrix was decreased [13, 22, 29]. As shown in Table 7, the impact damage of concrete containing 0.75% RTSF was slightly lower than that of other RTSF reinforced concrete mixtures, implying that 0.75% RTSF can provide a better enhancement for concrete.

Fig. 13 demonstrates the stress-strain curves of all concrete specimens at strain rates of about $124.2\text{-}127.2 \text{ s}^{-1}$. At the same strain rate, the addition of RTSF increased the strain at peak stress and the ultimate strain of concrete, indicating a similar effect to that of ordinary manufactured steel fibres. Compared to RTSF0, the strain at peak stress of RTSF0.5, RTSF0.75, RTSF1.0 and RTSF1.25 was changed by about 4.8%, 6.0%, -0.9% and 5.9%, respectively at this strain rate, but was increased by 6.0-12.8%, 7.1-25.3%, 7.4-36.9% and 6.2-43.6%, respectively at other strain rates, which can be ascribed to the bridging effect of RTSF, leading to an enhanced deformation capacity of concrete. The stress can be transferred to both sides of the cracks to reduce stress concentration at the crack tip, thereby restricting the crack propagation [66].

The strain at peak stress of RTSF0.75 at different strain rates was found to be about 6.0-25.3% higher than that of RTSF0, while the peak strain of ISF1.0 was about 7.5-24.6% higher, suggesting that 0.75% would be the optimal volume fraction of RTSF (0.5-1.25%) in concrete.

3.6 Dynamic impact factor

3.6.1 Effect of strain rate

Fig. 14 shows the DIF of all concrete mixtures, which is defined as the ratio of dynamic compressive strength to static compressive strength of concrete. When the average strain rate was about 35 s^{-1} , the DIF values were less than 1, suggesting that the dynamic compressive strength of concrete was less than its static compressive strength. This is because the micro-cracks inside the concrete cannot

propagate immediately at a low strain rate, proving that the concrete was intact (see Table 7) and can continue to bear higher impact loading [73]. When the strain rate exceeded 55 s^{-1} , DIFs of all mixtures were higher than 1 and increased with increasing strain rates, which can be attributed to the gradually increasing dynamic compressive strength of concrete mixtures under impact loading. However, as the strain rate increased from 35 s^{-1} to 125 s^{-1} , the increment of DIF gradually decreased. The growth rate of dynamic compressive strength of concrete decreased almost linearly with the increasing strain rate. It can be clearly observed that the size and number of cracks in concrete were small at a relatively low strain rate, and the fibres inside can effectively restrain the crack propagation. However, at high strain rates, a large number of micro-cracks could occur and propagate rapidly, thus reducing the effect of fibres and the bridging action of steel fibres [68]. It was reported that DIF of mixtures had a linear relation with the logarithm of strain rate [74]. Fig. 15 presents the linear fitting curves of DIF against the logarithm of the corresponding strain rate of different concrete mixtures. The fitting degree of DIFs and strain rates can be measured by the correlation coefficient R^2 that are given in Table 9. For all mixtures, the values of R^2 are all greater than 0.9, indicating a high reliability of the fitting curve.

3.6.2 Effect of RTSF content

Fig. 16 shows the effect of RTSF content on DIF of all concrete mixtures. The DIFs at various strain rates were increased first and reached the maximum value when the volume fraction of RTSF reached 0.75%, but then declined with the further incorporation of RTSF until the RTSF dosage reached 1%. The DIF values of RTSF1.25 at average strain rates of about 35 s^{-1} , 55 s^{-1} , 110 s^{-1} and 125 s^{-1} were lower than that of RTSF1.0 but exceeded that of RTSF1.0 at strain rates of 75 s^{-1} and 95 s^{-1} and became the maximum compared to other mixtures at the same strain rate. This can be attributed to the combined effect of dynamic and static compressive strengths [49]. At the strain rates of 75 s^{-1} and 95 s^{-1} , the decrease of static compressive strength of RTSF1.25 relative to RTSF1.0 (5.1%) was greater than the decrease of dynamic compressive strength, i.e., 0.2% and 3.0%, respectively. Besides, the DIFs of RTSF0.75 were increased by 5.6-8.8% compared to that of RTSF0 under different strain rates and varied from -1.6-2.3% relative to that of ISF1.0, indicating that 0.75% RTSF and 1.0% ISF exhibited similar effects on the DIFs of mixtures. Therefore, in combination with static compressive strength, dynamic compressive strength and DIF, the optimal volume fraction of RTSF can be considered as 0.75% for RTSF reinforced concrete.

3.7 Energy dissipation

3.7.1 Effect of strain rate

The fracture energy is defined as the energy absorbed by concrete up to peak stress under dynamic loading, while the total energy represents the total energy absorbed by concrete in both pre-peak and post-peak regions. The fracture energy and total energy at various strain rates of all concrete mixtures are shown in Figs. 17 and 18, respectively. It can be observed that the fracture energy and total energy were increased with increasing strain rate, indicating they both had strain rate effect. The fracture energy of RTSF0.5, RTSF0.75, RTSF1.0, RTSF1.25 and ISF1.0 was respectively increased by 14.6-29.3%, 21.8-62.5%, 14.9-44.6%, 13.6-31.8% and 12.3-44.8% compared to RTSF0 at different strain rates, while the total energy was improved by 2.1-18.8%, 21.0-29.6%, 26.4-50.1%, 6.1-18.3% and 18.5-32.5%, respectively. The increasing energy dissipation can be explained by the fact that the increasing strain rates generated more micro-cracks, and crack propagation required more energy. During the whole damage process of concrete, in addition to the energy needed to fracture the concrete, it also took additional amount of energy to overcome the toughness of the fibres and to pull fibres out of the concrete matrix across the fracture zone.

3.7.2 Effect of RTSF content

Figs. 19 and 20 show the effects of RTSF content on fracture energy and total energy of concrete, which were increased first until reaching the maximum value with the increase of RTSF content to 0.75% and then decreased, indicating a similar trend to static and dynamic compressive strengths. The fracture energy of RTSF0.75 at different strain rates was increased by 38.5%, 37.1%, 20.3%, 40.5%, 51.1%, and 29.7%, respectively, while the total dissipated energy was increased by 37.9%, 50.1%, 30.0%, 26.4%, 34.1%, and 39.6%, respectively in comparison with that of RTSF0. As the total dissipated energy of FRC is composed of the energy needed to generate cracks and the energy to pull the fibres out, the energy dissipation effect of concrete was increased with the enhanced bonding effect between fibre and concrete matrix. As shown in Table 7, RTSF reinforced concrete looked more complete compared to RTSF0, implying the increase of dissipated energy of concrete due to the bridging action of RTSF in concrete. Also, it can be seen from Table 8 that the dissipated energy of the post-cracking zone of the same concrete at different strain rates was higher than the fracture energy. Fig. 21 shows the proportion of fracture energy and energy absorbed in post-cracking zone of RTSF0.75. For the strain rate ranging from 34.9 s^{-1} to 127.2 s^{-1} , the dissipated energy in the

post-cracking zone of RTSF0, RTSF0.5, RTSF0.75, RTSF1.0, and RTSF1.25 was respectively about 2.5-83.8%, 10.1-45.3%, 1.6-51.9%, 3.2-48.8%, and 7.7-72.1% higher than the fracture energy. This can be explained by the fact that the energy in the post-cracking zone was mainly used to pull out the steel fibres or overcome the bridging action of the fibres in concrete. Interfacial interaction between fibres and concrete matrix, anchorage length and fibre shape are the main factors influencing the dissipated energy for fibres [75]. In addition, the cracks in concrete propagated rapidly under impact loading, and the bonding effect between fibre and concrete matrix increased, leading to an enhanced energy dissipation ability of concrete.

With the same fibre dosage (1.0%), the fracture energy and total energy of RTSF1.0 and ISF1.0 were consistently close at different strain rates. The change ranges of the fracture energy and total energy of RTSF1.0 relative to ISF1.0 were -3.3-6.7% and -4.9-11.3%, respectively. At different strain rates, the fracture energy and total energy of RTSF0.75 were about 3.9-12.5% and 0.4-25.7% higher than that of ISF1.0, respectively. As seen in Fig. 10, the number of fibres across the cracks in RTSF0.75 was significantly more than that of ISF1.0. The curved shape of RTSF led to a relatively high mechanical anchoring force between RTSF and concrete matrix, and at the same time formed a higher friction force with the matrix during the pull-out process [62]. In addition, RTSF with different lengths exhibited a combined effect in concrete. The short fibres in RTSF reinforced concrete mainly inhibited the initiation of micro-cracks and then were gradually pulled out with the propagation of micro-cracks, while the long fibres began to inhibit the cracks, which prolonged the damage of concrete and increased the dissipated energy of concrete. Considering the dissipated energy, 0.75% can be regarded as the optimal volume dosage of RTSF in concrete.

4. Conclusions

In this study, the workability and static and dynamic compressive strengths of recycled tyre steel fibre (RTSF) reinforced concrete were investigated, with a special emphasis on the effects of fibre content (0.5%, 0.75%, 1.0% and 1.25%) and strain rate (35, 55, 75, 95, 110 and 125 s⁻¹) on dynamic compressive behaviour. For comparisons, the specimens of concrete without steel fibre and concrete reinforced with 1.0% industrial steel fibre (ISF) were prepared and used as reference specimens. According to the experimental results, the main conclusions can be drawn as follows:

- With the increase of RTSF content, the slump of concrete decreased, while the air content increased. For RTSF and ISF reinforced concrete with the same fibre content (1.0%) but different

fibre shape and aspect ratio, the slump and air content of RTSF1.0 were 17.4% and 15.3% respectively higher than that ISF1.0, indicating that the fibre shape and aspect ratio have a great influence on the workability and quality of concrete.

- As the content of RTSF increased from 0 to 0.75%, the static compressive strength and dynamic compressive strength of concrete at various strain rates were significantly improved. However, with the further increase of RTSF content from 0.75% to 1.25%, both the static and dynamic compressive strengths began to decrease but were still higher than that of RTSF0. Under impact loading, RTSF were pulled out from concrete matrix with the propagation of cracks, leading to an increase in the dynamic compressive strength of concrete.
- All mixtures with various fibre contents were sensitive to strain rate, the dynamic compressive strength and energy dissipation capacity of which were increased with increasing strain rate. There existed a good correlation between the dynamic increase factor (DIF) and strain rate, as indicated by the correlation coefficients of fitting curves of DIF changing with the logarithm of strain rate, which are all greater than 0.9 for different mixtures.
- Considering workability, compressive strength, and dynamic compressive performance, the optimal dosage of RTSF for concrete was 0.75%. The workability of RTSF0.75 met the construction requirements, the static and dynamic compressive strengths of which were 25.0% and 17.6-25.1% respectively higher than that of RTSF0. Compared to RTSF0, the fracture energy and total energy of RTSF0.75 were 29.7-51.1% and 26.4-39.6% respectively higher. 1.0% ISF can be replaced by 0.75% RTSF for concrete, considering its workability, compressive strength, and dynamic compressive performance.
- The bond between RTSF and concrete matrix was highly dependent on the fibre length and shape. Therefore, the effect of RTSF with different length distribution on workability and mechanical properties of concrete needs to be further explored. This is the subject of ongoing work and will be presented in a future publication.

Acknowledgements

M. Chen would like to thank the Natural Science Foundation of Liaoning Province (No. 2020-MS-089) and Fundamental Research Funds for the Central Universities (No. N2001005), China for financial support. M. Zhang gratefully acknowledges the financial support from the Engineering and Physical Sciences Research Council (EPSRC), UK under Grant No. EP/R041504/1 and the Royal

Society, UK under Award No. IEC\NSFC\191417 as well as the Visiting Researcher Fund Program of State Key Laboratory of Water Resources and Hydropower Engineering Science, China under Award No. 2019SGG01.

References

- [1] A. Bentur, S. Mindess, *Fibre reinforced cementitious composites*, Crc Press 2006.
- [2] A. Caggiano, P. Folino, C. Lima, E. Martinelli, M. Pepe, On the mechanical response of hybrid fiber reinforced concrete with recycled and industrial steel fibers, *Construction and Building Materials* 147 (2017) 286-295.
- [3] A.P. Wadekar, R. Pandir, Study of different types fibres used in high strength fibre reinforced concrete, *Inno. Res. in Ad. Engg.* 1 (2014) 225-30.
- [4] J.-L. Granju, S.U. Balouch, Corrosion of steel fibre reinforced concrete from the cracks, *Cement and Concrete Research* 35(3) (2005) 572-577.
- [5] I. Havlikova, I. Merta, A. Schneemayer, V. Vesely, H. Šimonová, B. Korycanska, Z. Kersner, Effect of fibre type in concrete on crack initiation, *Applied Mechanics and Materials*, Trans Tech Publ, 2015, pp. 308-311.
- [6] E. Arunakanthi, J.C. Kumar, Experimental studies on fiber reinforced concrete (FRC), *International Journal of Civil Engineering and Technology* 7(5) (2016) 329-336.
- [7] N.F. Medina, D.F. Medina, F. Hernández-Olivares, M. Navacerrada, Mechanical and thermal properties of concrete incorporating rubber and fibres from tyre recycling, *Construction and Building Materials* 144 (2017) 563-573.
- [8] M.A. Aiello, F. Leuzzi, Waste tyre rubberized concrete: Properties at fresh and hardened state, *Waste management* 30(8-9) (2010) 1696-1704.
- [9] A. Sofi, Effect of waste tyre rubber on mechanical and durability properties of concrete—A review, *Ain Shams Engineering Journal* 9(4) (2018) 2691-2700.
- [10] G. Malarvizhi, N. Senthul, C. Kamaraj, A study on Recycling of crumb rubber and low density polyethylene blend on stone matrix asphalt, *International Journal of Science and Research* 2(10) (2012).
- [11] S. Gigli, D. Landi, M. Germani, Cost-benefit analysis of a circular economy project: a study on a recycling system for end-of-life tyres, *Journal of Cleaner Production* 229 (2019) 680-694.

- [12] R. Andrei, L. Dumitrescu, S.G. Maxineasa, Using Recycled Components from Post-Consumer Tyres in Construction Materials Industry, 14th INTERNATIONAL MULTIDISCIPLINARY SCIENTIFIC GEOCONFERENCE SGEM 2014, 2014, pp. 259-264.
- [13] M. Mastali, A. Dalvand, A. Sattarifard, M. Illikainen, Development of eco-efficient and cost-effective reinforced self-consolidation concretes with hybrid industrial/recycled steel fibers, *Construction and Building Materials* 166 (2018) 214-226.
- [14] K. Kotresh, M.G. Belachew, Study on waste tyre rubber as concrete aggregates, *International Journal of Scientific Engineering and Technology* 3(4) (2014) 433-436.
- [15] M. Chen, H. Zhong, L. Chen, Y. Zhang, M. Zhang, Engineering properties and sustainability assessment of recycled fibre reinforced rubberised cementitious composite, *Journal of Cleaner Production* 278 (2021) 123996.
- [16] T.S. Vadivel, R. Thenmozhi, M. Doddurani, Experimental behaviour of waste tyre rubber aggregate concrete under impact loading, *Iranian Journal of Science and Technology. Transactions of Civil Engineering* 38(C1+) (2014) 251.
- [17] E. Martinelli, A. Caggiano, H. Xargay, An experimental study on the post-cracking behaviour of Hybrid Industrial/Recycled Steel Fibre-Reinforced Concrete, *Construction and Building Materials* 94 (2015) 290-298.
- [18] M.A. Aiello, F. Leuzzi, G. Centonze, A. Maffezzoli, Use of steel fibres recovered from waste tyres as reinforcement in concrete: Pull-out behaviour, compressive and flexural strength, *Waste Management* 29 (2009) 1960–1970.
- [19] M. Ahmadi, S. Farzin, A. Hassani, M. Motamedi, Mechanical properties of the concrete containing recycled fibers and aggregates, *Construction and Building Materials* 144 (2017) 392-398.
- [20] M. Papadrakakis, V. Papadopoulos, G. Stefanou, V. Plevris, MESO-SCALE MODELING OF HYBRID INDUSTRIAL/RECYCLED STEEL FIBER-REINFORCED CONCRETE.
- [21] O. Onuaguluchi, N. Banthia, Scrap tire steel fiber as a substitute for commercial steel fiber in cement mortar: engineering properties and cost-benefit analyses, *Resources, Conservation and Recycling* 134 (2018) 248-256.
- [22] H. Hu, P. Papastergiou, H. Angelakopoulos, M. Guadagnini, K. Pilakoutas, Mechanical properties of SFRC using blended manufactured and recycled tyre steel fibres, *Construction and Building Materials* 163 (2018) 376-389.

- [23] M. Leone, G. Centonze, D. Colonna, F. Micelli, M.A. Aiello, Experimental Study on Bond Behavior in Fiber-Reinforced Concrete with Low Content of Recycled Steel Fiber, *Journal of Materials in Civil Engineering* 28(04016068) (2016).
- [24] M. Leone, G. Centonze, D. Colonna, F. Micelli, M. Aiello, Fiber-reinforced concrete with low content of recycled steel fiber: Shear behaviour, *Construction and Building Materials* 161 (2018) 141-155.
- [25] A. Baricevic, D. Bjegovic, M. Skazlic, Hybrid fiber–reinforced concrete with unsorted recycled-tire steel fibers, *Journal of materials in civil engineering* 29(6) (2017) 06017005.
- [26] J. Domski, J. Katzer, M. Zakrzewski, T. Ponikiewski, Comparison of the mechanical characteristics of engineered and waste steel fiber used as reinforcement for concrete, *Journal of Cleaner Production* 158 (2017) 18-28.
- [27] C. Frazão, B. Díaz, J. Barros, J.A. Bogas, F. Toptan, An experimental study on the corrosion susceptibility of Recycled Steel Fiber Reinforced Concrete, *Cement and Concrete Composites* 96 (2019) 138-153.
- [28] G. Centonze, M. Leone, M.A. Aiello, Steel fibers from waste tires as reinforcement in concrete: A mechanical characterization, *Construction and Building Materials* 36 (2012) 46-57.
- [29] M.N. Isa, K. Pilakoutas, M. Guadagnini, H. Angelakopoulos, Mechanical performance of affordable and eco-efficient ultra-high performance concrete (UHPC) containing recycled tyre steel fibres, *Construction and Building Materials* 255 (2020).
- [30] K.B. Najim, A. Saeb, Z. Al-Azzawi, Structural behaviour and fracture energy of recycled steel fibre self-compacting reinforced concrete beams, *Journal of Building Engineering* 17 (2018) 174-182.
- [31] M. Mastali, A. Dalvand, A. Sattarifard, Z. Abdollahnejad, M. Illikainen, Characterization and optimization of hardened properties of self-consolidating concrete incorporating recycled steel, industrial steel, polypropylene and hybrid fibers, *Composites Part B: Engineering* 151 (2018) 186-200.
- [32] Ł. Skarżyński, J. Suchorzewski, Mechanical and fracture properties of concrete reinforced with recycled and industrial steel fibers using Digital Image Correlation technique and X-ray micro computed tomography, *Construction and Building Materials* 183 (2018) 283-299.

- [33] M. Mastali, A. Dalvand, Fresh and hardened properties of self-compacting concrete reinforced with hybrid recycled steel–polypropylene fiber, *Journal of Materials in Civil Engineering* 29(6) (2017) 04017012.
- [34] D.-Y. Yoo, N. Banthia, Impact resistance of fiber-reinforced concrete–A review, *Cement and Concrete Composites* 104 (2019) 103389.
- [35] M.R. Khosravani, K. Weinberg, A review on split Hopkinson bar experiments on the dynamic characterisation of concrete, *Construction and Building Materials* 190 (2018) 1264-1283.
- [36] N. Li, Z. Jin, G. Long, L. Chen, Q. Fu, Y. Yu, X. Zhang, C. Xiong, Impact resistance of steel fiber-reinforced self-compacting concrete (SCC) at high strain rates, *Journal of Building Engineering* 38 (2021) 102212.
- [37] J. Xiao, K. Zhang, Q. Zhang, Strain rate effect on compressive stress–strain curves of recycled aggregate concrete with seawater and sea sand, *Construction and Building Materials* 300 (2021) 124014.
- [38] S. Gurusideswar, A. Shukla, K.N. Jonnalagadda, P. Nanthagopalan, Tensile strength and failure of ultra-high performance concrete (UHPC) composition over a wide range of strain rates, *Construction and Building Materials* 258 (2020) 119642.
- [39] W. Feng, F. Liu, F. Yang, L. Li, L. Jing, B. Chen, B. Yuan, Experimental study on the effect of strain rates on the dynamic flexural properties of rubber concrete, *Construction and Building Materials* 224 (2019) 408-419.
- [40] AC, Design Considerations for Steel Fiber Reinforced Concrete, *ACI Struct J* 1988 85.
- [41] M. Mastali, A. Dalvand, Use of silica fume and recycled steel fibers in self-compacting concrete (SCC), *Construction and Building Materials* 125 (2016) 196–209.
- [42] A.H. Farhan, A.R. Dawson, N.H. Thom, Recycled hybrid fiber-reinforced & cement-stabilized pavement mixtures: Tensile properties and cracking characterization, *Construction and Building Materials* 179 (2018) 488–499.
- [43] K. Aghaee, M.A. Yazdi, K.D. Tsavdaridis, Investigation into the mechanical properties of structural lightweight concrete reinforced with waste steel wires, *Magazine of Concrete Research* (2014).
- [44] S.-C. Lee, J.-H. Oh, J.-Y. Cho, Compressive Behavior of Fiber-Reinforced Concrete with End-Hooked Steel Fibers, *materials* (2015) 1442-1458.

- [45] Standard for test method of performance on ordinary fresh concrete, GB/T50080-2016, China Academy of Building Research, China, 2016.
- [46] Standard for test method of mechanical properties on ordinary concrete, GB/T50081-2002, China Academy of Building Research, China, 2002.
- [47] Y.B. Lu, Q.M. Li, Appraisal of pulse-shaping technique in split Hopkinson pressure bar tests for brittle materials, *Protective Structures 1* (2010) 363-389.
- [48] R. Naghdabadi, M.J. Ashrafi, A. J., Experimental and numerical investigation of pulse-shaped split Hopkinson pressure bar test, *Materials Science & Engineering A* 539 (2012) 285-293.
- [49] M. Chen, W. Chen, H. Zhong, D. Chi, Y. Wang, M. Zhang, Experimental study on dynamic compressive behaviour of recycled tyre polymer fibre reinforced concrete, *Cement and Concrete Composites* 98 (2019) 95–112.
- [50] H. Zhong, M. Zhang, Experimental study on engineering properties of concrete reinforced with hybrid recycled tyre steel and polypropylene fibres, *Journal of Cleaner Production* 259(120914) (2020).
- [51] K.H. Younis, Metakaolin modified recycled aggregate concrete containing recycled steel fibers, *Materials Today: Proceedings* (2021).
- [52] O. Sengul, Mechanical behavior of concretes containing waste steel fibers recovered from scrap tires, *Construction and Building Materials* 122 (2016) 649–658.
- [53] R. Yu, P. Spiesz, H.J.H. Brouwers, Static properties and impact resistance of a green Ultra-High Performance Hybrid Fibre Reinforced Concrete (UHPHFRC): Experiments and modeling, *Construction and Building Materials* 68 (2014) 158-171.
- [54] A. Cladera, B. Weber, C. Leinenbach, C. Czaderski, M. Shahverdi, M. Motavalli, Iron-based shape memory alloys for civil engineering structures: An overview, *Construction and Building Materials* 63 (2014) 281-293.
- [55] M. Chen, H. Zhong, M. Zhang, Flexural fatigue behaviour of recycled tyre polymer fibre reinforced concrete, *Cement and Concrete Composites* 105 (2020) 103441.
- [56] J. Wang, Q. Dai, R. Si, S. Guo, Mechanical, durability, and microstructural properties of macro synthetic polypropylene (PP) fiber-reinforced rubber concrete, *Journal of Cleaner Production* 234 (2019) 1351-1364.

- [57] A. Kostrzanowska-Siedlarz, J.J.C. Go?Aszewski, B. Materials, Rheological properties and the air content in fresh concrete for self compacting high performance concrete, 94 (2015) 555-564.
- [58] T. Uygunođlu, Effect of fiber type and content on bleeding of steel fiber reinforced concrete, *Construction and Building Materials* 25 (2011) 766-772.
- [59] Z. Wu, C. Shi, W. He, L. Wu, Effects of steel fiber content and shape on mechanical properties of ultra high performance concrete, *Construction and Building Materials* 103 (2016) 8-14.
- [60] A.R. Khaloo, A. Esrafilı, M. Kalani, M.H. Mobini, Use of polymer fibres recovered from waste car timing belts in high performance concrete, *Construction and Building Materials* 80 (2015) 31-37.
- [61] M.F. Smrkic, D. Damjanović, A. Baricevic, Application of recycled steel fibres in concrete elements subjected to fatigue loading, *Gradevinar* 69 (10) (2017) 893-905.
- [62] Y. Hao, H. Hao, Dynamic compressive behaviour of spiral steel fibre reinforced concrete in split Hopkinson pressure bar tests, *Construction and Building Materials* 48 (2013) 521–532.
- [63] X. Hou, S. Cao, W. Zheng, Q. Rong, G. Li, Experimental study on dynamic compressive properties of fiber-reinforced reactive powder concrete at high strain rates, *Engineering Structures* 169 (2018) 119–130.
- [64] L. Jin, R. Zhang, Y. Tian, G. Dou, X. Du, Experimental investigation on static and dynamic mechanical properties of steel fiber reinforced ultra-high-strength concretes, *Construction and Building Materials* 178 (2018) 102-111.
- [65] Q. Li, X. Zhao, S. Xu, X. Gao, Influence of steel fiber on dynamic compressive behavior of hybrid fiber ultra high toughness cementitious composites at different strain rates, *Construction and Building Materials* 125 (2016) 490-500.
- [66] X. Hou, S. Cao, Q. Rong, W. Zheng, G.J.C. Li, B. Materials, Effects of steel fiber and strain rate on the dynamic compressive stress-strain relationship in reactive powder concrete, *Construction Building Materials* 170 (2018) 570-581.
- [67] G.M. Ren, H. Wu, Q. Fang, J.Z. Liu, Effects of steel fiber content and type on dynamic compressive mechanical properties of UHPCC, *Construction and Building Materials* 164 (2018) 29-43.
- [68] Y. Wang, Z. Wang, X. Liang, M. An, Experimental and numerical studies on dynamic compressive behavior of reactive powder concretes, *Acta Mechanica Solida Sinica* 21(5) (2008) 420-430.

- [69] M.Q. Li, H. Meng, About the dynamic strength enhancement of concrete-like materials in a split Hopkinson pressure bar test, *International Journal of Solids and Structures* 40 (2003) 343–360.
- [70] S. Wang, H.T.N. Le, L.H. Poh, S.T. Quek, M.-H. Zhang, Effect of high strain rate on compressive behavior of strain-hardening cement composite in comparison to that of ordinary fiber-reinforced concrete, *Construction and Building Materials* 136 (2017) 31-43.
- [71] P.H. Bischoff, S.H.J.M. Perry, Structures, Compressive behaviour of concrete at high strain rates, *Materials and Structures* 24(6) (1991) 425-450.
- [72] H. Zhang, L. Wang, K. Zheng, B.T. Jibrin, P.G. Totakhil, Research on compressive impact dynamic behavior and constitutive model of polypropylene fiber reinforced concrete, *Construction and Building Materials* 187 (2018) 584–595.
- [73] Y.S. Tai, Uniaxial compression tests at various loading rates for reactive powder concrete, *Theoretical Applied Fracture Mechanics* 52 (2009) 14-21.
- [74] Z. Wu, C. Shi, W. He, D. Wang, Static and dynamic compressive properties of ultra-high performance concrete (UHPC) with hybrid steel fiber reinforcements, *Cement and Concrete Composites* 79 (2017) 148-157.
- [75] Z. Wu, K.H. Khayat, C. Shi, How do fiber shape and matrix composition affect fiber pullout behavior and flexural properties of UHPC?, *Cement and Concrete Composites* 90 (2018) 193-201.

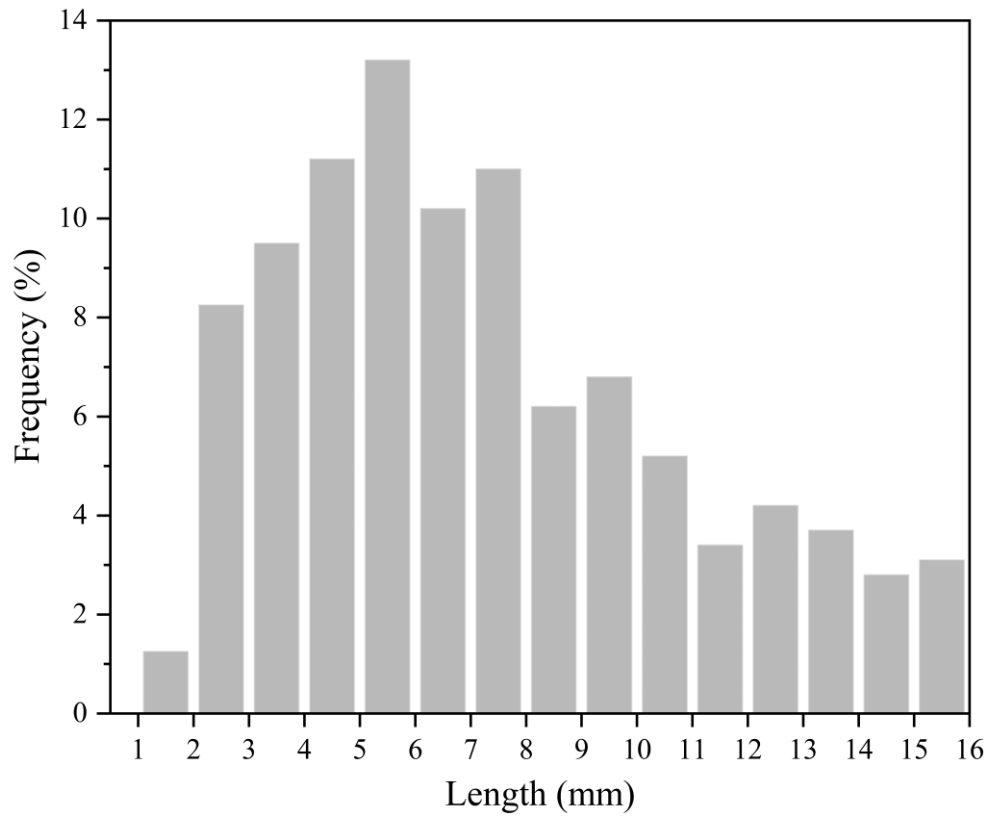


Fig. 1. Length distribution of recycled tyre steel fibre (RTSF).

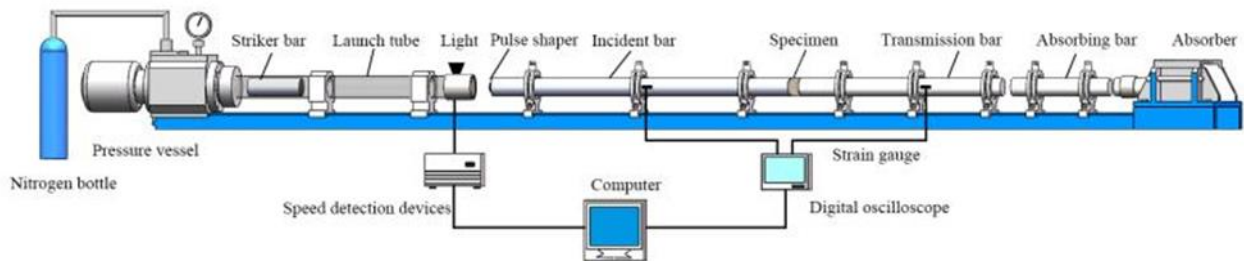


Fig. 2. Splitting Hopkinson pressure bar (SHPB) testing system.

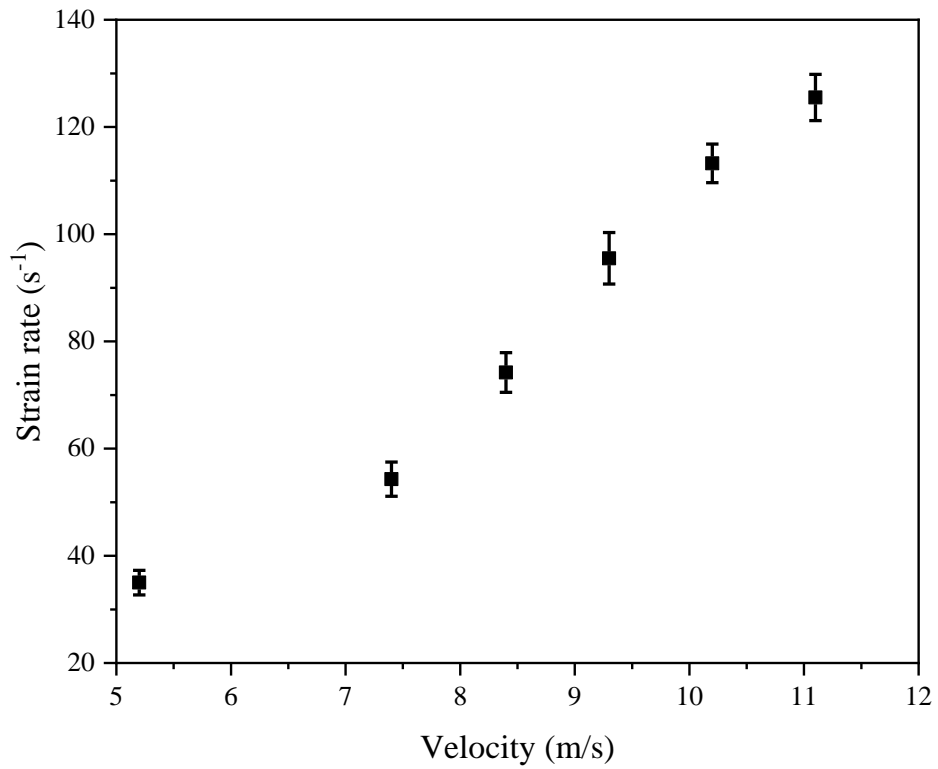


Fig. 3. Relationship between velocity of striker bar and strain rate for RTSF0 mixture.

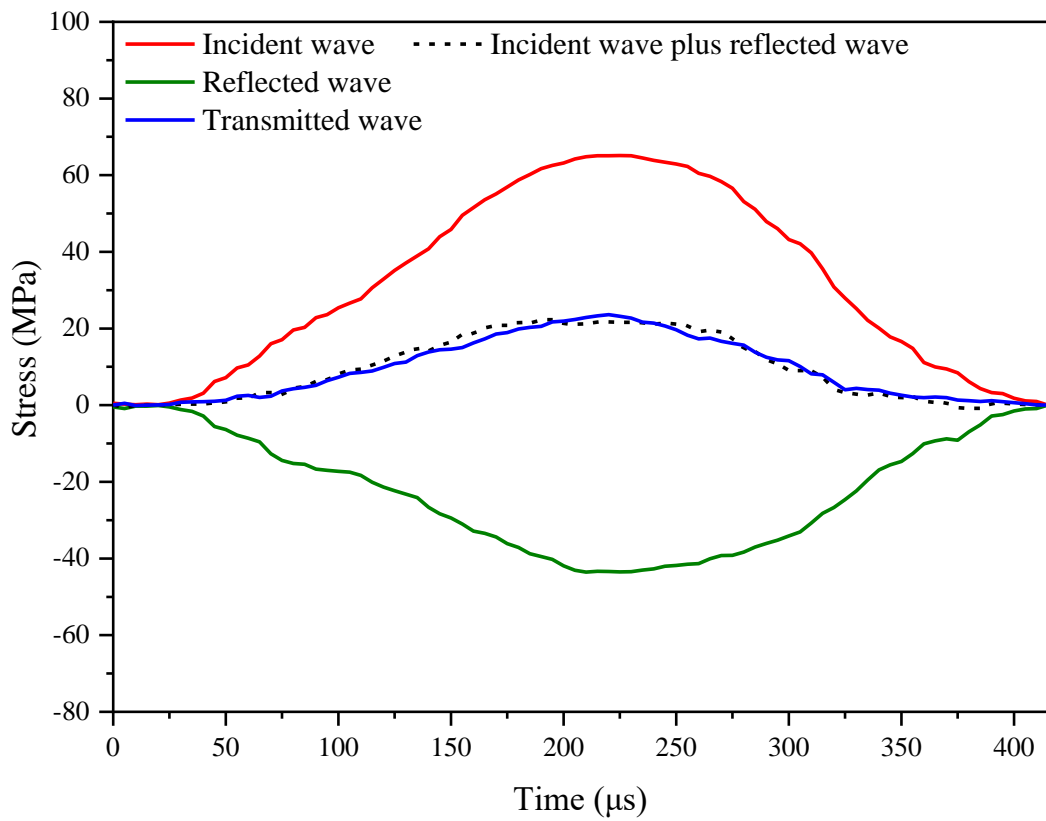


Fig. 4. Validation of the stress equilibrium during the SHPB test.

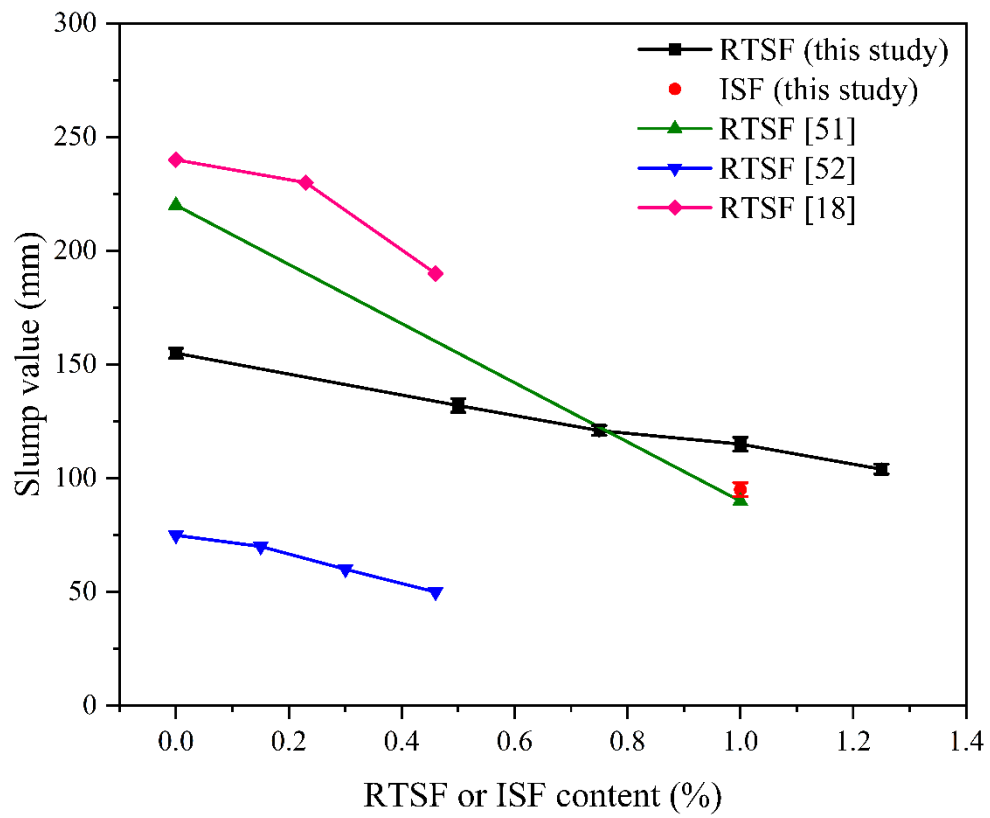


Fig. 5. Effect of fibre on slump of concrete.

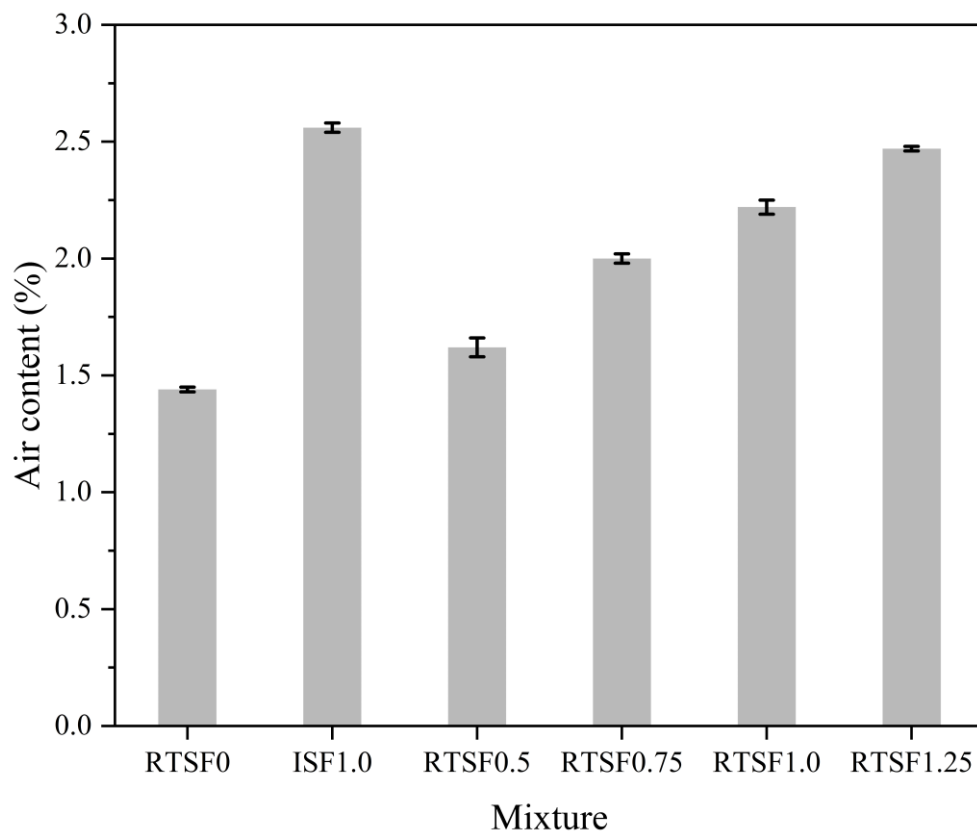


Fig. 6. Effect of fibre on air content of concrete.

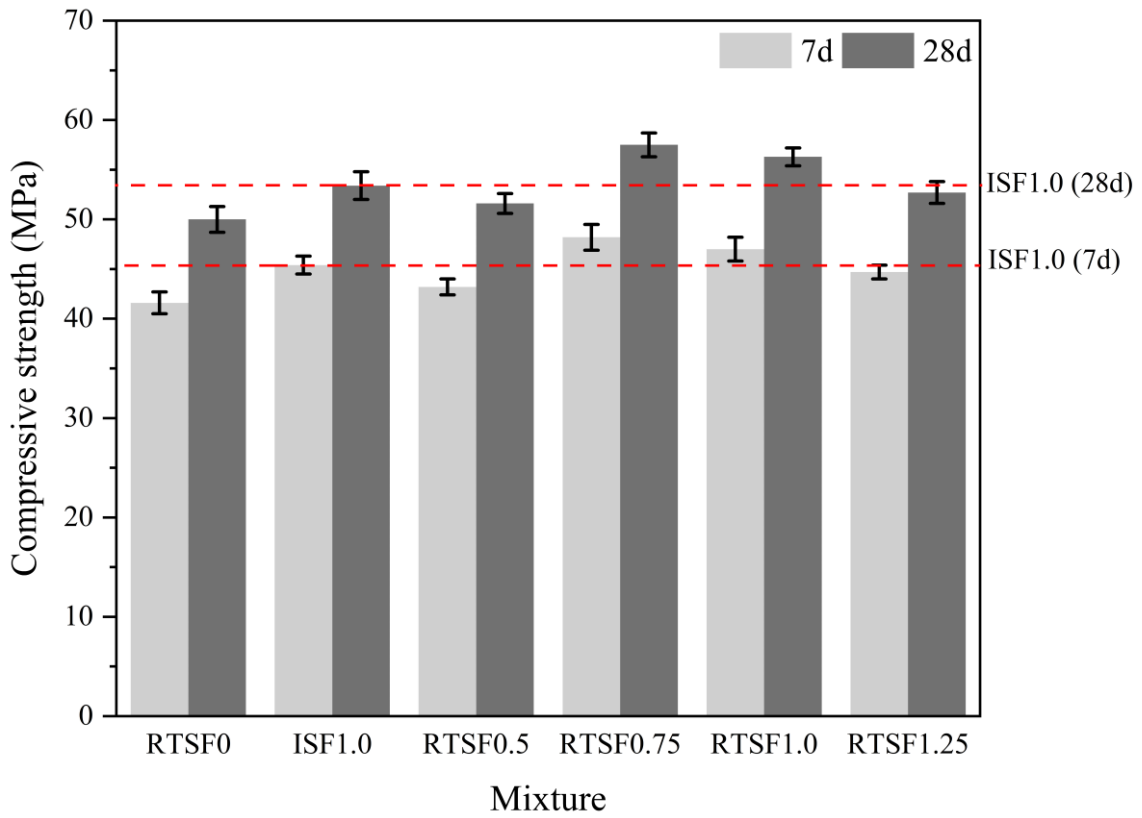


Fig. 7. Compressive strength of all mixtures at 7 d and 28 d.

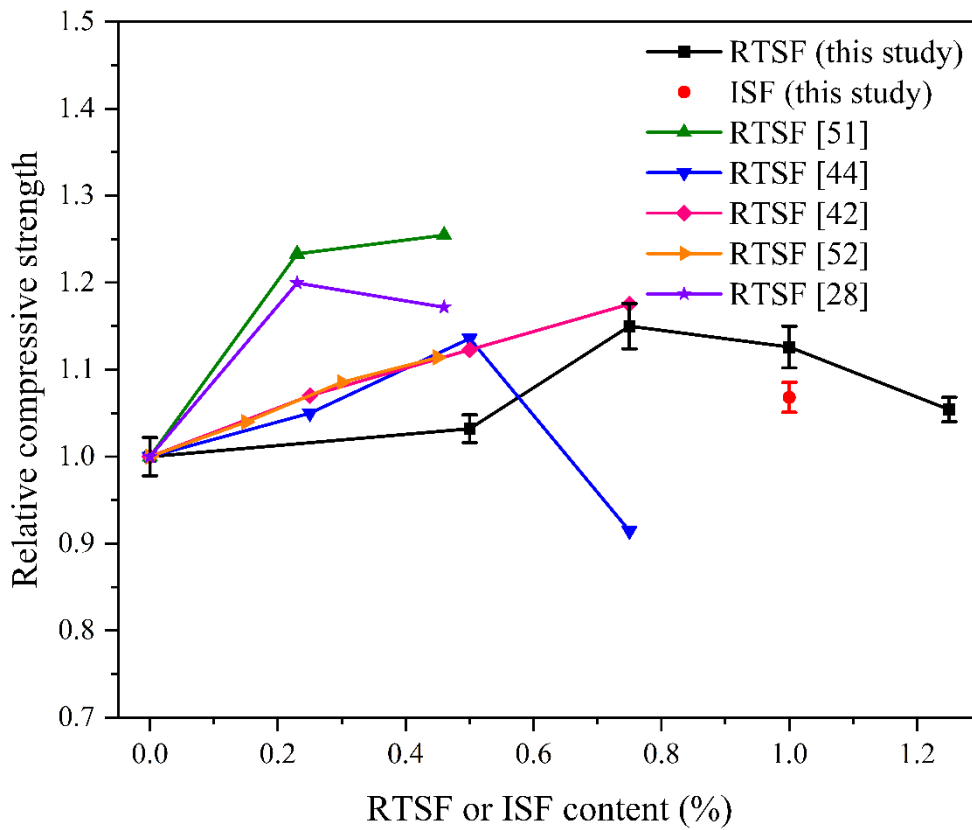


Fig. 8. Effect of RTSF content on compressive strength of concrete.

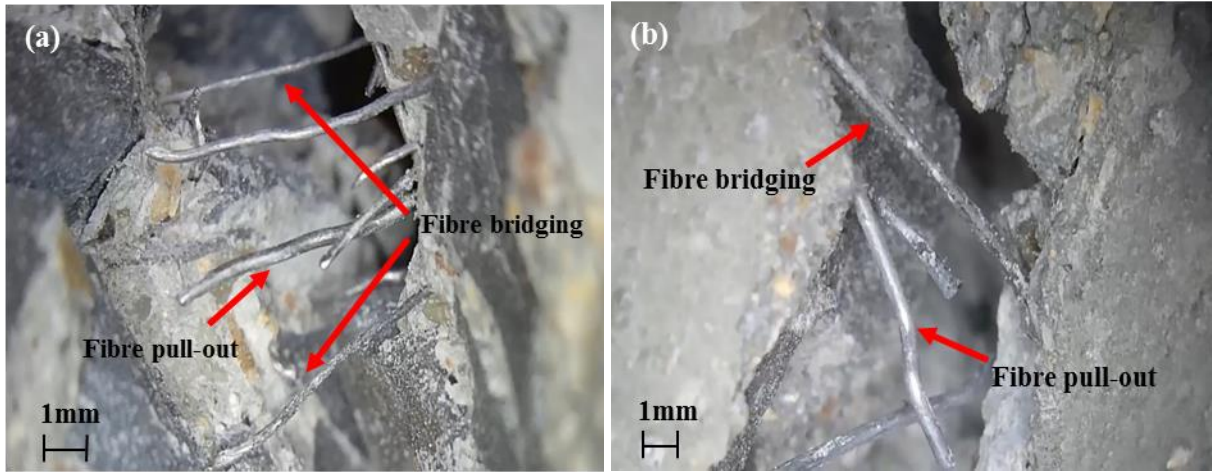


Fig. 9. Fracture surface: (a) RTSF0.75, (b) ISF1.0.

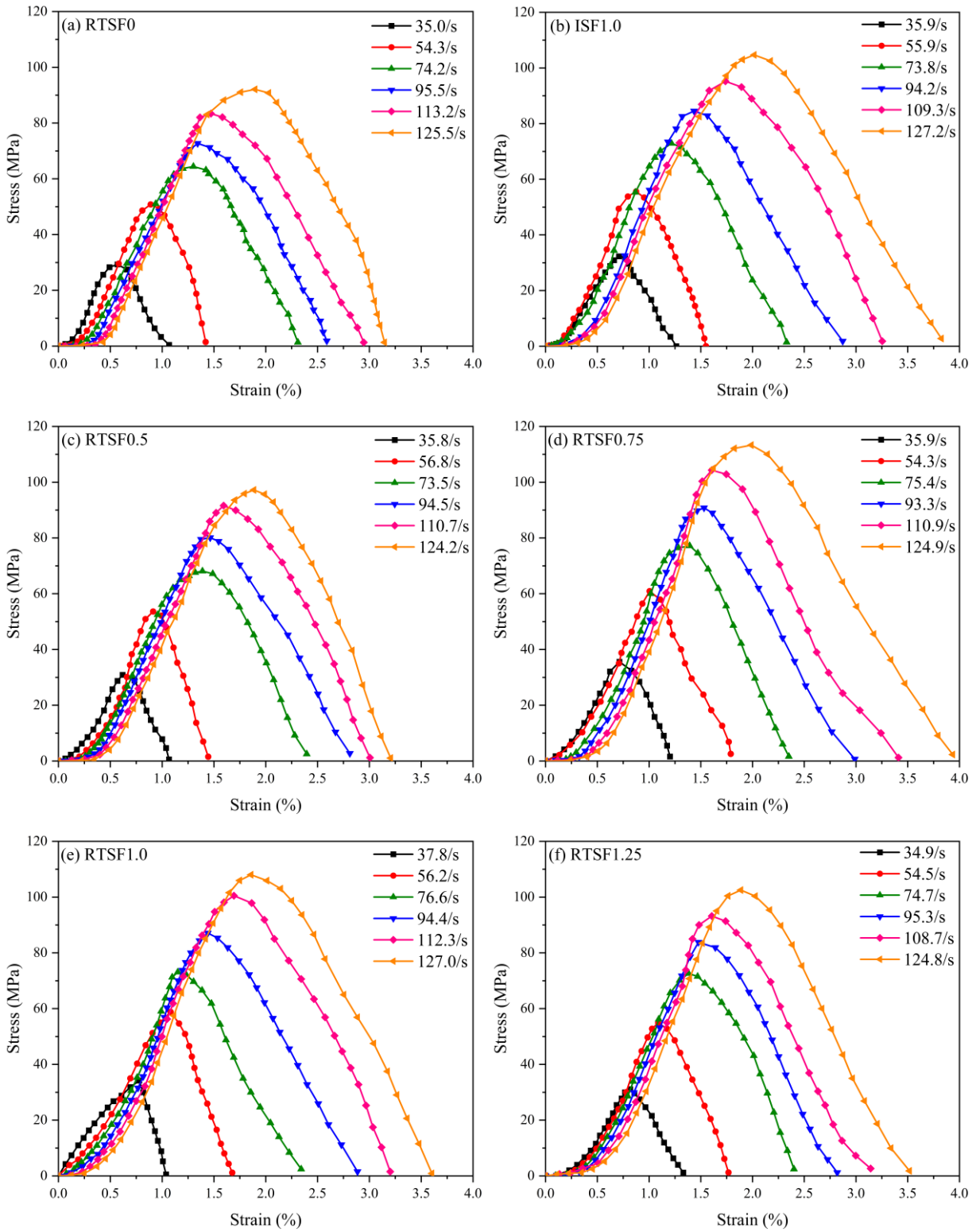


Fig. 10. Effect of strain rate on dynamic compressive stress-strain response of: (a) RTSF0, (b) ISF1.0, (c) RTSF0.5, (d) RTSF0.75, (e) RTSF1.0, and (f) RTSF1.25.

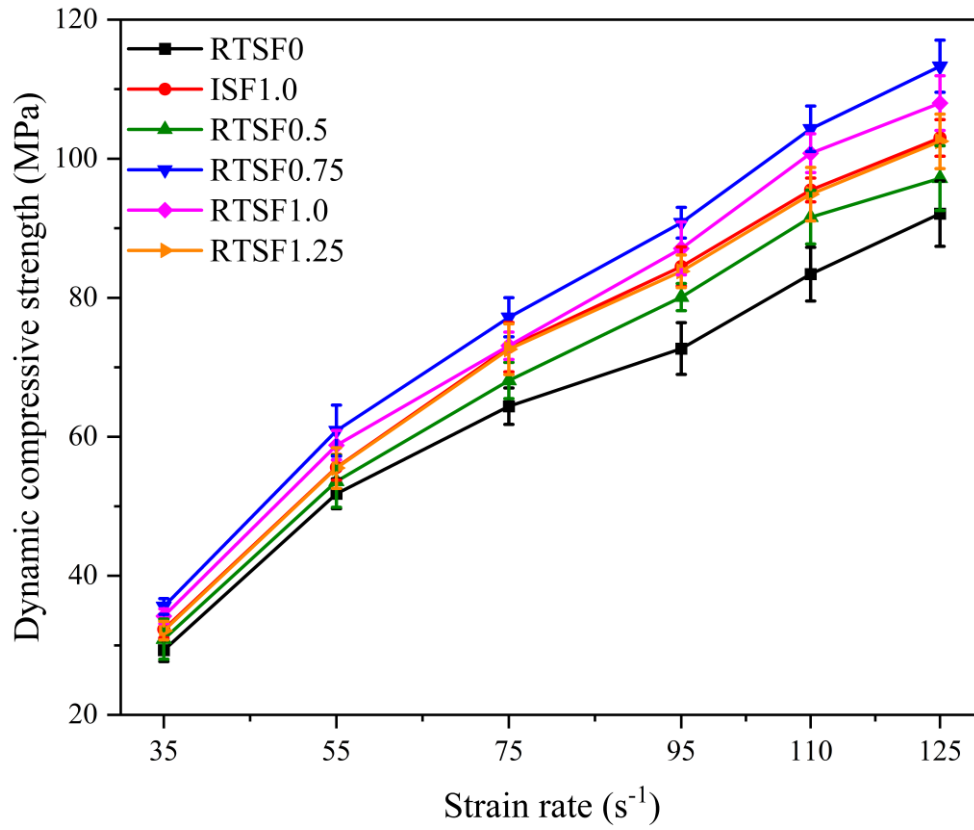


Fig. 11. Effect of strain rate on dynamic compressive strength of RTSF / ISF reinforced concrete.

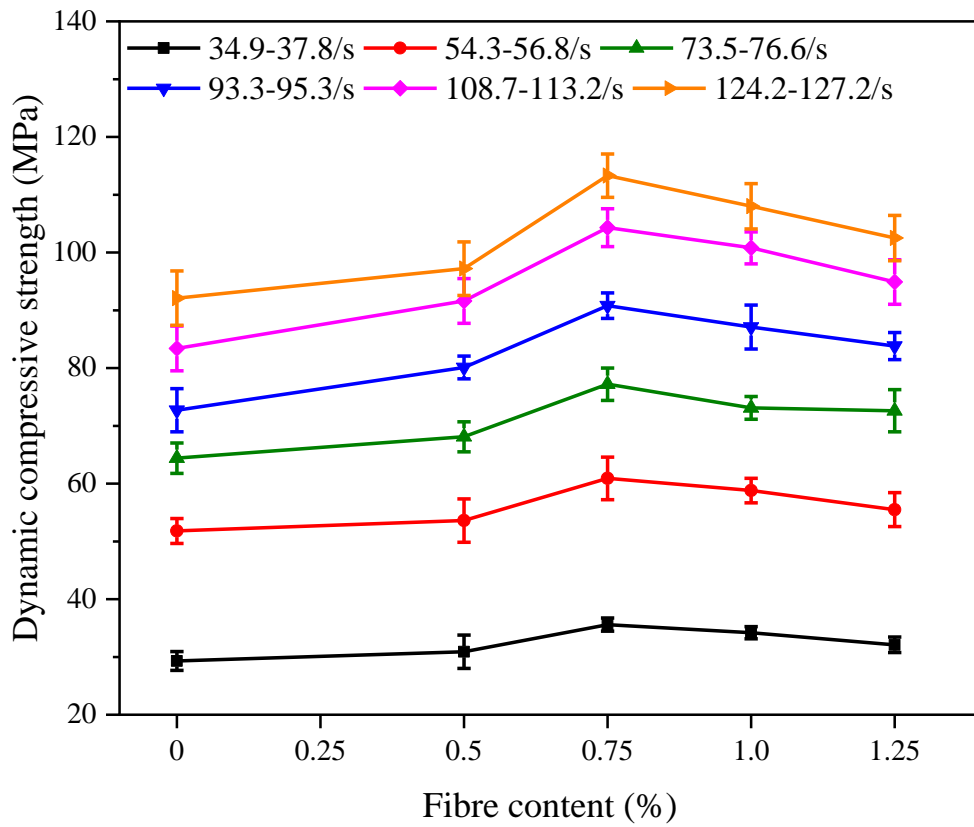


Fig. 12. Effect of RTSF content on dynamic compressive strength of concrete.

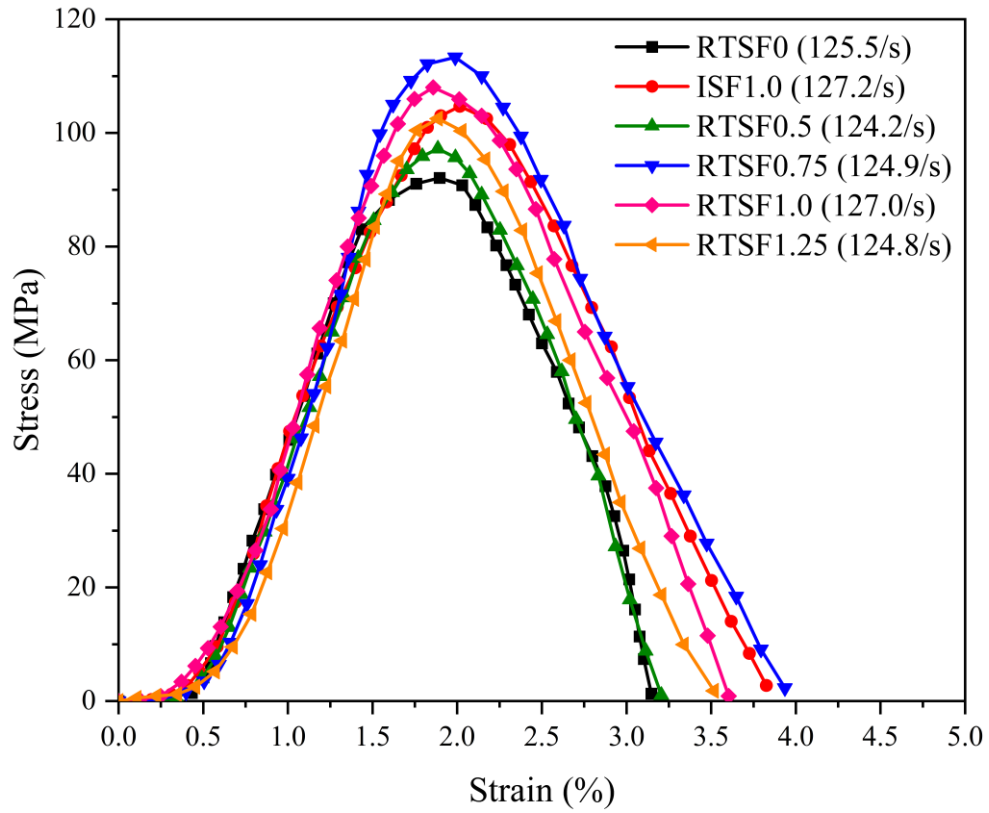


Fig. 13. Effect of RTSF and ISF on stress-strain response of concrete at a strain rate of 120 s^{-1} .

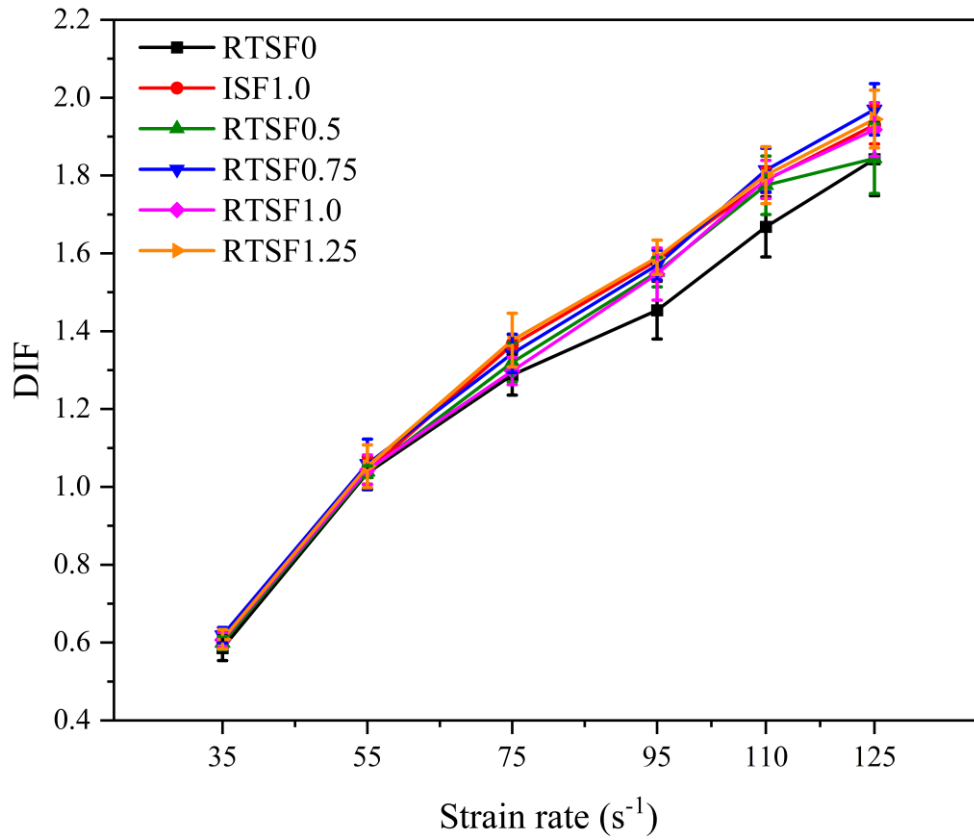


Fig. 14. Effect of strain rate on DIF of RTSF and ISF reinforced concrete.

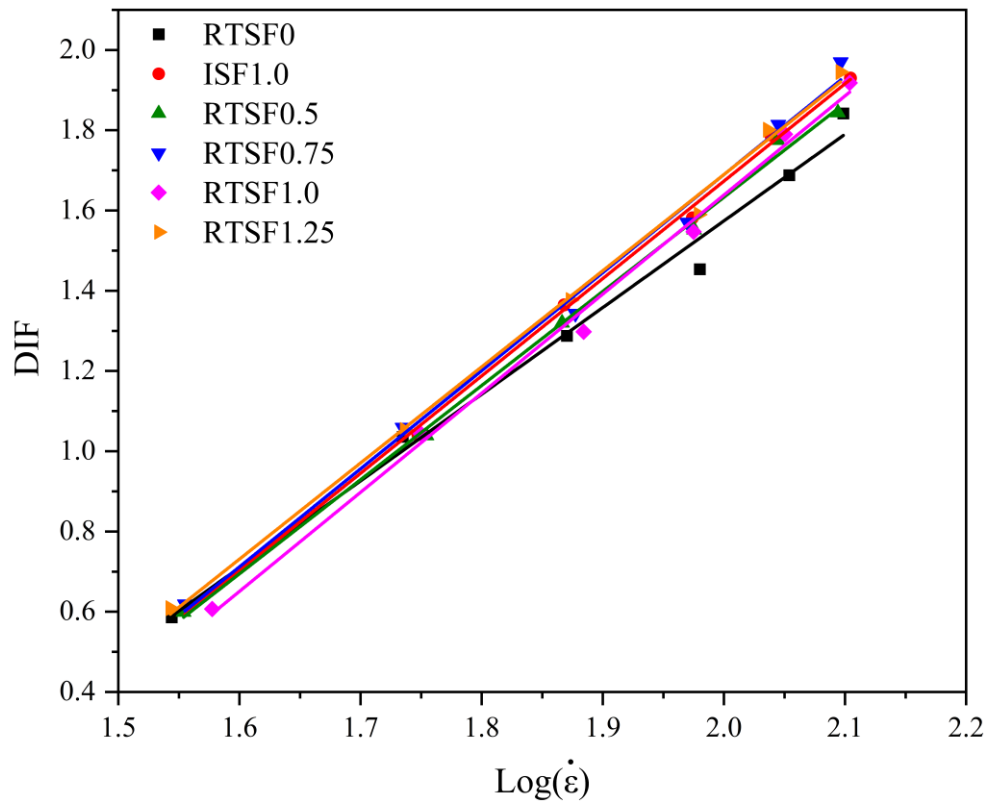


Fig. 15. Relationship between DIF and strain rate ($\dot{\epsilon}$) for all mixtures.

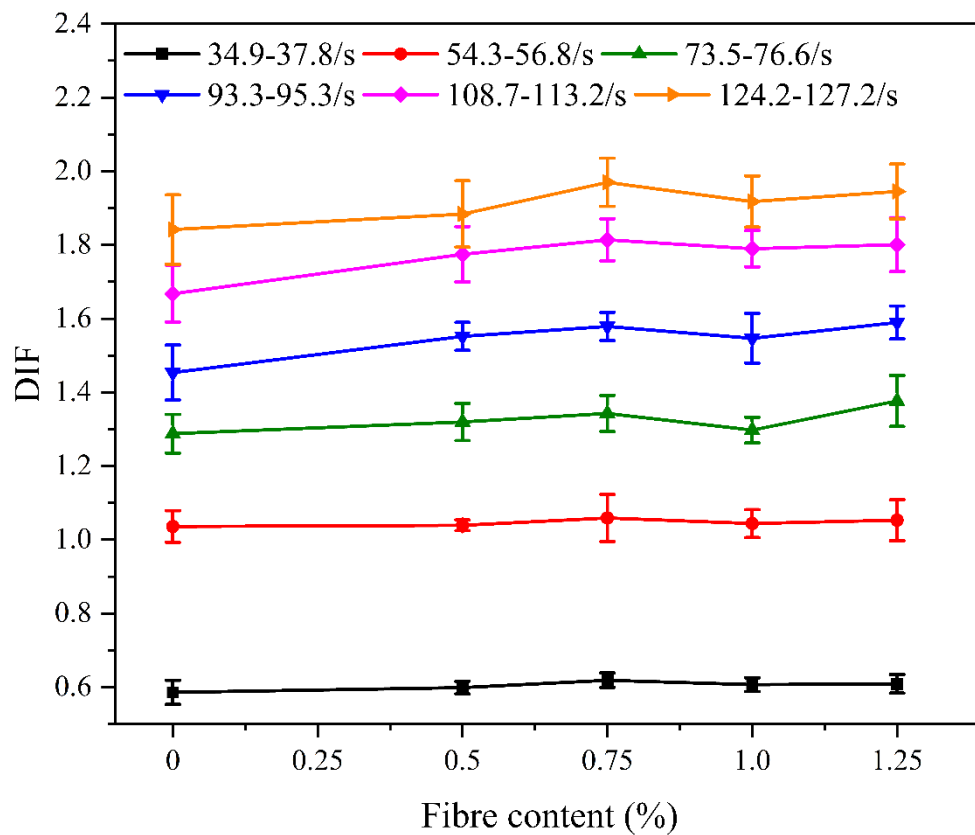


Fig. 16. Effect of RTSF content on DIF of concrete at various strain rates.

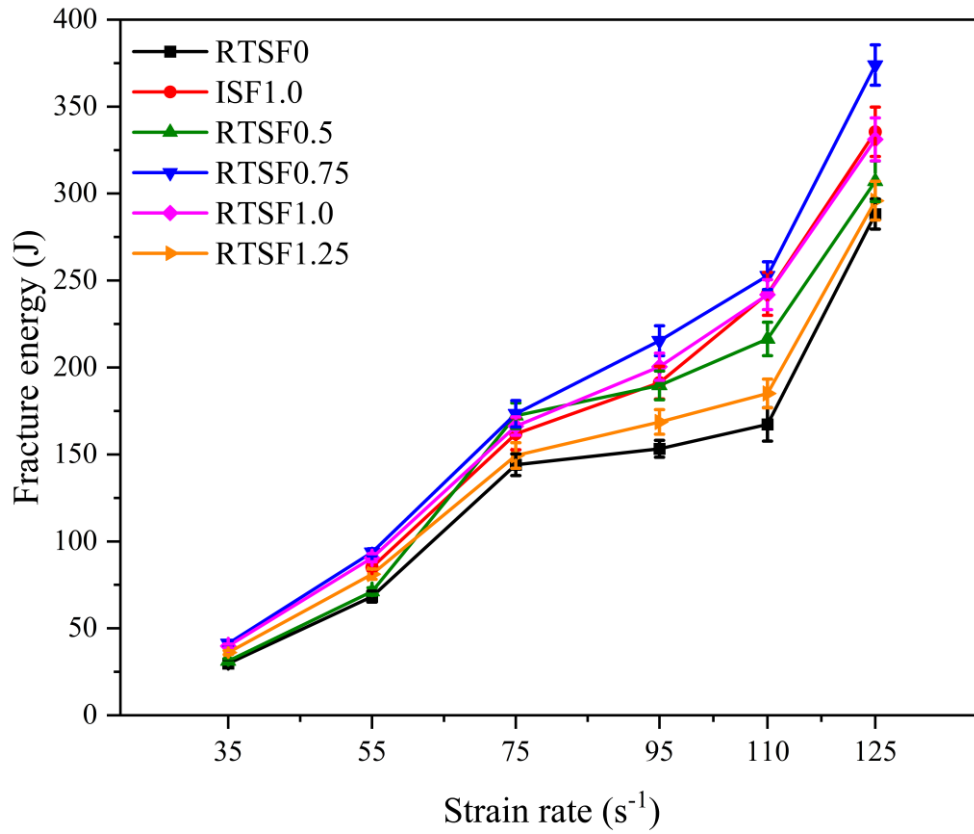


Fig. 17. Effect of strain rate on fracture energy of RTSF and ISF reinforced concrete.

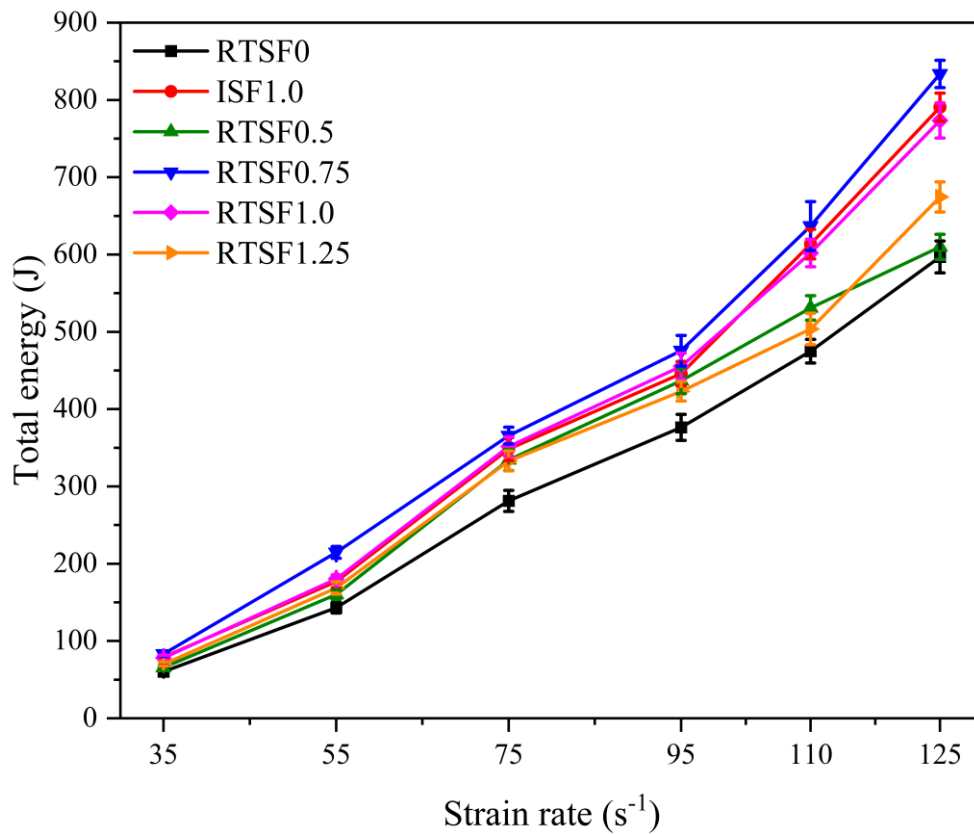


Fig. 18. Effect of strain rate on total energy of RTSF and ISF reinforced concrete.

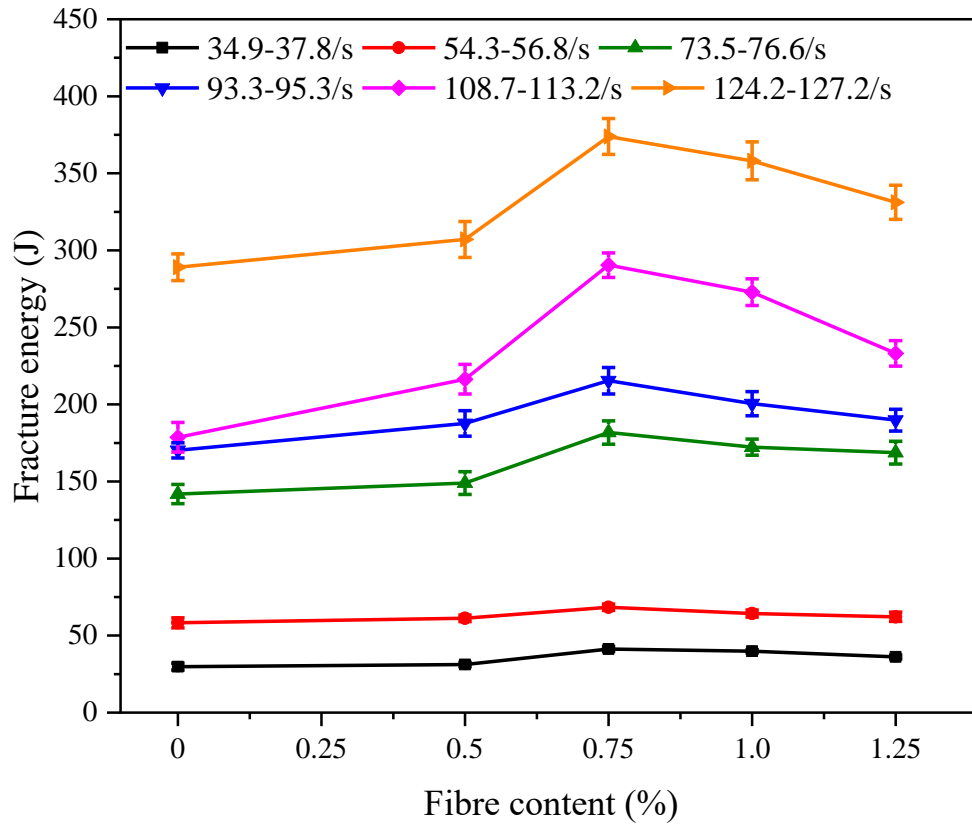


Fig. 19. Effect of RTSF content on fracture energy of concrete at various strain rates.

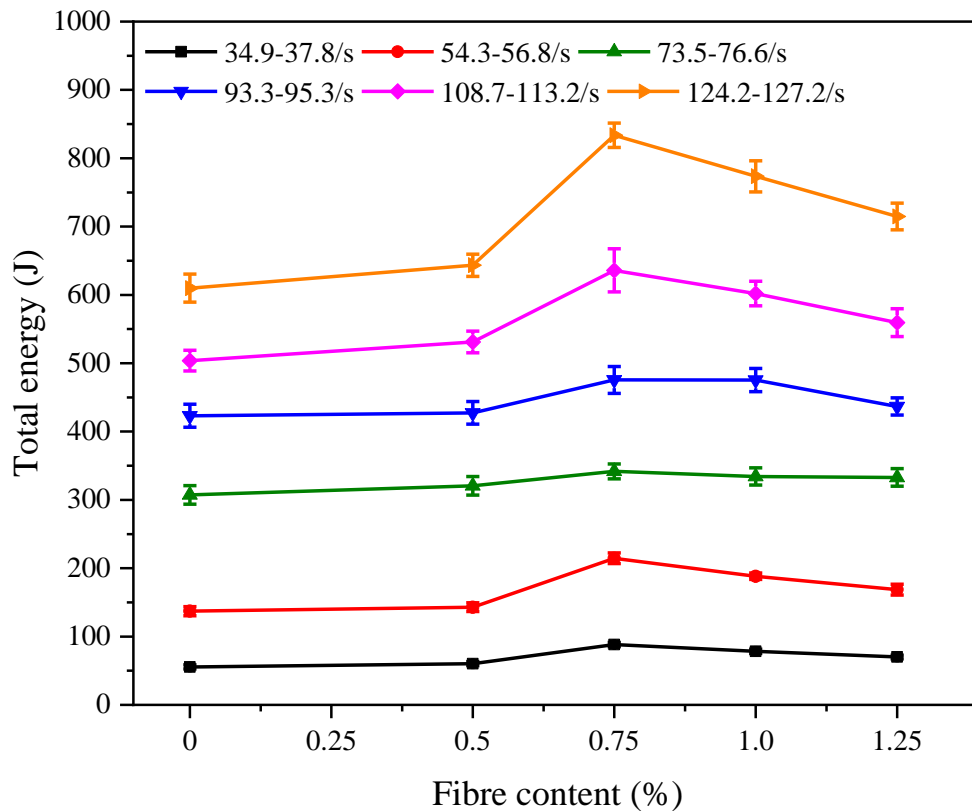


Fig. 20. Effect of RTSF content on total energy of concrete at various strain rates.

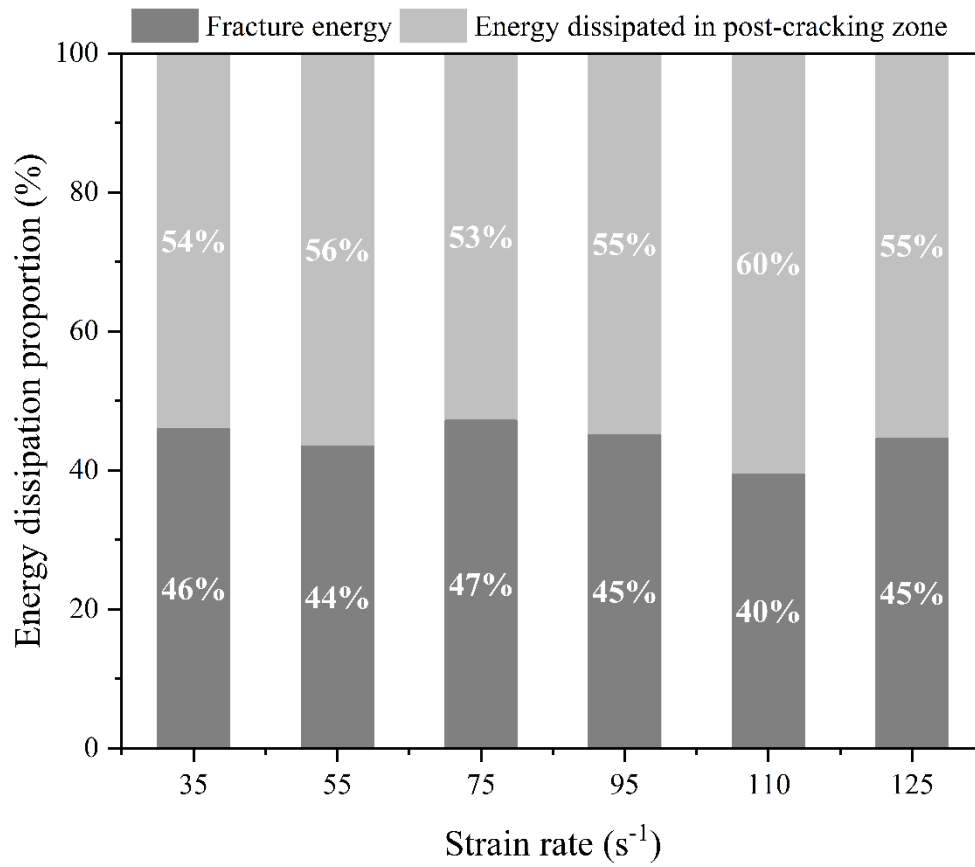


Fig. 21. Proportion of fracture energy and energy dissipated in post-cracking zone of RTSF0.75.

Table 1 Chemical composition (wt%) of cement.

Oxide	CaO	SiO ₂	Al ₂ O ₃	Fe ₂ O ₃	MgO	SO ₃	Na ₂ O	LOI
Cement	60.56	21.35	5.98	2.91	2.22	2.05	0.21	4.72

Note: LOI (Loss on Ignition).



Table 2 Particle size distribution of fine aggregate.

Sieve size (mm)	Percentage passing (%)
0.15	7.7
0.3	34
0.6	25.4
1.18	14.0
2.36	12.9
4.75	2.7

Table 3 Properties of coarse aggregate used in this study.

Apparent density (kg/m ³)	Packing density (kg/m ³)	Void fraction (%)	Silt content (%)	Needle flake content (%)	Crushing index (%)
2675	1598	35	0.29	2	6.5

Table 4 Geometry and properties of fibres used in this study.

Fibre type	Fibre morphology	Length (mm)	Diameter (mm)	Tensile strength (MPa)	Elastic modulus (GPa)
ISF		35	0.54	1345	220
RTSF		1.4~15.6	0.22	2165	200

Note: ISF (Industrial steel fibre), RTSF (Recycled tyre steel fibre).

Table 5 Mix proportions of specimens (kg/m³).

Symbol	Cement	FA	CA	Water	SP	ISF	RTSF	V _f (%)	
								ISF	RTSF
RTSF0	477	485	1283	200	4	0	0	/	/
ISF1.0	477	485	1283	200	4	78	0	1.0	/
RTSF0.5	477	485	1283	200	4	0	39	/	0.5
RTSF0.75	477	485	1283	200	4	0	59	/	0.75
RTSF1.0	477	485	1283	200	4	0	78	/	1.0
RTSF1.25	477	485	1283	200	4	0	98	/	1.25

Note: FA (fine aggregate), CA (coarse aggregate), SP (superplasticiser).

Table 6 Number of specimens for each test and each strain rate.

Symbol	Type of test		Strain rate (s ⁻¹)					
	Static compressive strength test	Dynamic compressive strength test	35	55	75	95	110	125
RTSF0	6	18	3	3	3	3	3	3
ISF1.0	6	18	3	3	3	3	3	3
RTSF0.5	6	18	3	3	3	3	3	3
RTSF0.75	6	18	3	3	3	3	3	3
RTSF1.0	6	18	3	3	3	3	3	3
RTSF1.25	6	18	3	3	3	3	3	3

Table 7 Failure patterns of all mixtures at various strain rates.

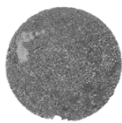

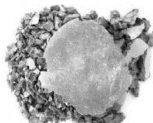




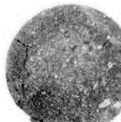
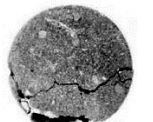
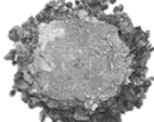
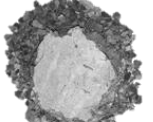
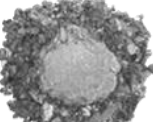





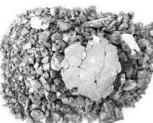
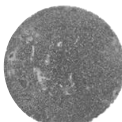
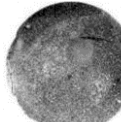
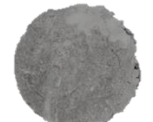

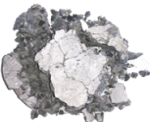
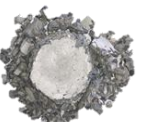

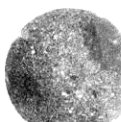
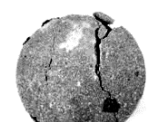


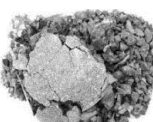
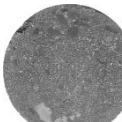
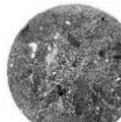
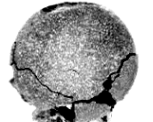
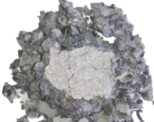
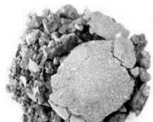

Symbol	Strain rate (s^{-1})					
	35	55	75	95	110	125
RTSF0						
ISF1.0						
RTSF0.5						
RTSF0.75						
RTSF1.0						
RTSF1.25						

Table 8 Summary of dynamic properties of RTSF or ISF reinforced concrete obtained from SHPB test.

Symbol	Compressive strength (MPa)	Average strain rate (s ⁻¹)	Maximum dynamic stress (MPa)	Strain at peak stress (×10 ⁻³)	Ultimate strain (×10 ⁻³)	DIF	Fracture energy (J)	Total energy (J)
RTSF0	50.03 ± 2.43	35.0	29.30 ± 1.63	5.69	10.27	0.59 ± 0.03	29.82 ± 2.23	60.41 ± 2.86
		54.3	51.82 ± 2.15	8.29	14.00	1.04 ± 0.04	68.31 ± 3.26	143.02 ± 6.68
		74.2	64.43 ± 2.62	13.01	22.70	1.29 ± 0.05	144.13 ± 6.25	281.31 ± 13.62
		95.5	72.71 ± 3.73	13.42	26.09	1.45 ± 0.07	153.34 ± 4.86	376.32 ± 16.81
		113.2	83.45 ± 3.87	14.11	29.45	1.67 ± 0.08	167.32 ± 9.63	474.93 ± 15.23
		125.5	92.16 ± 4.71	18.76	31.46	1.84 ± 0.09	288.23 ± 8.66	596.92 ± 20.61
ISF1.0	53.46 ± 0.86	35.9	32.32 ± 1.22	7.09	13.06	0.61 ± 0.02	38.62 ± 2.12	79.23 ± 2.19
		55.9	55.63 ± 1.85	9.35	15.34	1.04 ± 0.03	85.12 ± 1.87	176.95 ± 8.61
		73.8	72.92 ± 3.56	12.37	23.77	1.37 ± 0.01	161.92 ± 9.19	348.32 ± 14.93
		94.2	84.53 ± 2.82	14.35	28.72	1.58 ± 0.05	191.31 ± 9.36	446.03 ± 15.77
		109.3	95.52 ± 1.71	17.38	32.54	1.79 ± 0.03	242.32 ± 12.36	613.51 ± 19.22
		127.2	103.02 ± 2.63	20.16	38.26	1.93 ± 0.05	335.51 ± 14.20	790.72 ± 18.12
RTSF0.5	51.62 ± 0.71	35.8	30.92 ± 2.88	6.18	10.46	0.60 ± 0.02	31.23 ± 1.43	65.62 ± 2.95
		56.8	53.63 ± 3.75	8.34	14.06	1.04 ± 0.02	71.22 ± 2.13	160.13 ± 6.31
		73.5	68.12 ± 2.61	13.89	23.96	1.32 ± 0.05	172.32 ± 7.38	334.32 ± 13.61
		94.5	80.15 ± 1.96	14.64	29.12	1.55 ± 0.04	189.75 ± 8.27	436.73 ± 16.65
		110.7	91.62 ± 3.87	15.93	30.06	1.78 ± 0.08	216.43 ± 9.61	531.04 ± 15.85
		124.2	97.25 ± 4.65	18.85	32.06	1.84 ± 0.09	307.1 ± 11.63	609.92 ± 16.25
RTSF0.75	57.58 ± 1.31	35.9	35.62 ± 1.13	7.13	10.52	0.62 ± 0.02	41.32 ± 1.62	83.32 ± 3.12
		54.3	60.96 ± 3.68	10.05	17.89	1.06 ± 0.06	93.72 ± 2.06	214.63 ± 7.68
		75.4	77.25 ± 2.81	13.93	23.51	1.34 ± 0.05	173.43 ± 7.55	365.82 ± 10.86
		93.3	90.82 ± 2.20	15.31	29.88	1.57 ± 0.04	215.42 ± 8.63	475.62 ± 19.63
		110.9	104.33 ± 3.27	16.05	34.11	1.81 ± 0.06	252.82 ± 7.96	636.91 ± 31.62
		124.9	113.32 ± 3.75	19.88	39.35	1.97 ± 0.07	373.91 ± 11.63	833.72 ± 17.78
RTSF1.0	56.31 ± 2.45	37.8	34.21 ± 1.06	7.79	10.18	0.61 ± 0.02	39.82 ± 1.05	78.31 ± 3.11

Symbol	Compressive strength (MPa)	Average strain rate (s ⁻¹)	Maximum dynamic stress (MPa)	Strain at peak stress (×10 ⁻³)	Ultimate strain (×10 ⁻³)	DIF	Fracture energy (J)	Total energy (J)
		56.2	58.82 ± 2.13	10.12	16.76	1.04 ± 0.04	90.61 ± 2.31	180.22 ± 4.76
		76.6	73.12 ± 1.97	11.51	23.40	1.30 ± 0.04	166.32 ± 5.26	351.63 ± 12.69
		94.4	87.13 ± 3.81	14.41	28.86	1.55 ± 0.07	200.52 ± 7.81	455.42 ± 16.98
		112.3	100.82 ± 2.78	16.73	32.01	1.79 ± 0.05	241.92 ± 8.63	602.01 ± 17.91
		127.0	108.01 ± 3.93	18.58	36.04	1.92 ± 0.07	331.23 ± 12.32	773.53 ± 22.67
		34.9	32.12 ± 1.33	8.17	13.31	0.61 ± 0.03	36.12 ± 1.15	70.12 ± 2.63
		54.5	55.56 ± 2.93	10.88	17.67	1.05 ± 0.06	81.23 ± 2.95	168.72 ± 7.95
RTSF1.25	52.73 ± 1.76	74.7	72.62 ± 3.65	13.82	24.00	1.38 ± 0.07	149.42 ± 7.36	332.93 ± 12.85
		95.3	83.83 ± 2.35	14.77	28.19	1.59 ± 0.04	168.73 ± 7.11	423.14 ± 12.61
		108.7	94.96 ± 3.85	15.86	31.42	1.80 ± 0.07	185.12 ± 8.27	503.82 ± 20.36
		124.8	102.52 ± 3.91	18.87	35.17	1.95 ± 0.07	295.93 ± 11.13	674.54 ± 19.48

Table 9 Summary of the fitted DIF equations for different mixture.

Symbol	Fitted equation of DIF	R^2
RTSF0	$DIF=2.144\log(\hat{\epsilon})-2.718$	0.987
ISF1.0	$DIF=2.460\log(\hat{\epsilon})-3.238$	0.997
RTSF0.5	$DIF=2.350\log(\hat{\epsilon})-3.056$	0.996
RTSF0.75	$DIF=2.447\log(\hat{\epsilon})-3.202$	0.994
RTSF1.0	$DIF=2.469\log(\hat{\epsilon})-3.298$	0.994
RTSF1.25	$DIF=2.398\log(\hat{\epsilon})-3.105$	0.996